Symmetries of Composite Knots

by

John Matthew Mastin, Jr.

(Under the direction of Jason Cantarella)

Abstract

Prime knots and their symmetries have been studied and tabulated for more than a hundred years, but very little attention has been given to the tabulation of composite knots. We will develop a combinatorial strategy for tabulating composite knots and computing their symmetries knowing the symmetries of the prime factors. Along the way we will discuss the properties of an interesting combinatorial description of knot and link diagrams called the planar diagram code (PD-code). The PD-code exists in the literature [BN11], but there does not exist a formal discussion of their properties.

Symmetries of Composite Knots

by

John Matthew Mastin, Jr.

B.S. Southern Polytechnic State University, 2005

M.A. The University of Georgia, 2011

A Dissertation Submitted to the Graduate Faculty

of The University of Georgia in Partial Fulfillment

of the

Requirements for the Degree

Doctor of Philosophy

Athens, Georgia

2012

©2012

John Matthew Mastin, Jr.

All Rights Reserved

Symmetries of Composite Links

by

John Matthew Mastin, Jr.

Approved:

Major Professor: Jason Cantarella

Committee: Mike Usher
Joseph H.G Fu
David Gay

Electronic Version Approved:

Maureen Grasso
Dean of the Graduate School
The University of Georgia
August 2012

Acknowledgments

I would first like to thank Jason Cantarella for his friendship and advice during my entire graduate school career. I couldn't have asked for a better advisor. Secondly, I would like to thank Jason Parsley and Ryan Budney for many helpful conversations. Much of my support as a graduate student came from the National Science Foundation's VIGRE grant and the initial work that led to the theory developed in this thesis was started in a VIGRE research group at the University of Georgia. As such, I would also like to thank all of the members of the Knot Theory VIGRE group for their work on symmetry tabulation.

Without the support and patience of my wife Jennifer I don't believe this thesis would have been completed in my lifetime. Thank you for motivating me to keep working.

Contents

Chapter 1

Introduction

Link tabulation has a long history and many beautiful techniques have been developed to generate link tables. However, most of the standard tables are incomplete in the sense that they do not actually list representatives of each equivalence class of links (cf. Definition 2). For example, the Knot Atlas [BN11] lists only one trefoil (cf. Figure 1.1), but there are really *two* trefoils. The two trefoils are mirror images of one another in the sense that their isotopy classes are related by an orientation reversing diffeomorphism of S^3 (cf. Chapter 2). If one thinks about this too long it starts to become unclear why these two knots are related to each other. This will be discussed in more in Chapter 2. The question of how many different equivalence classes correspond to an entry in the current knot tables is related to the intrinsic symmetries of a knot. Whitten [WCW69] studied this type of symmetry in the late 1960s and has a beautiful theorem which gives necessary and sufficient conditions for a link to admit a given symmetry. Part of the motivation for the algebraic machine we will define is to compute the symmetries of a composite knot more easily than using the conditions given by Whitten. The current tables are also incomplete in the sense that they contain only prime knots (cf. Definition 4). There are two central results described in this thesis. The first is a combinatorial machine that can compute explicitly the intrinsic symmetries of composite

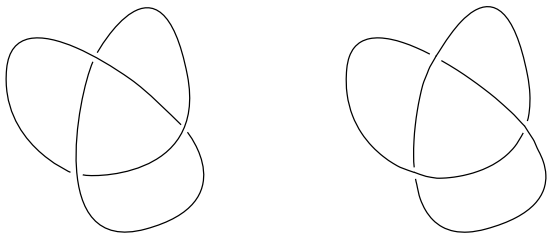

Figure 1.1: The two trefoils.

knots from the intrinsic symmetries of the prime factors (cf. Chapter 7). The second is an algorithm to generate complete tables of composite knots from the tables of prime knots and their symmetries (cf. Chapter 8).

In Chapter 3 we will discuss a combinatorial way to describe links. These objects, called PD-codes, appear in the literature [BN11], but there is currently no formal discussion of their properties. Chapters 4, 5, and 6 contain the technical details needed to justify the computation of symmetries of composites and the tabulation algorithm. The theory developed here is a step toward understanding the combinatorics of connected sums of links. While we only treat the case of knots in its entirety, we will provide an outline for the links case and discuss the obstructions to extending the theory.

Unless otherwise stated we will be working entirely within the smooth category.

Definition 1. An **isotopy** is a 1-parameter family of smooth embeddings. We say that two submanifolds X and Y of S^3 are **isotopic** if there is an isotopy $h : S^3 \to S^3$ such that $h_0(X) = X$ and $h_1(X) = Y$.

Definition 2. A μ component **link** in a 3-manifold M^3 is a smooth, oriented embedding of $\sqcup_\mu S^1 \to M^3$. The components are taken to be labeled and ordered by the set $\{1, \ldots, \mu\}$. A link with 1-component is called a **knot**. We say that two links L and L' in S^3 are equivalent, denoted $L \sim L'$ if they are isotopic.

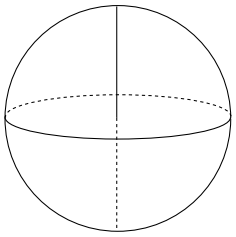

Figure 1.2: A trivial ball-arc pair.

1.1 Prime and Composite Links

We will now define prime links and discuss prime factorization.

Definition 3. An embedded $S^2 \to S^3$ is called an **admissible ball** with respect to a link L if its intersection with L is exactly two transverse points.

Definition 4. A knot or link L in S^3 is **prime** if exactly one side of any admissible ball is a trivial ball-arc-pair (i.e. isotopic to the configuration in Figure 1.2).

The decomposition of knots into prime factors was first studied by Schubert [Sch53] and later generalized to links by Hashizume [Has58]. Hashizume states this result as follows.

Theorem 5. *Every non-trivial and non-separable link can be decomposed uniquely into prime links.*

What this theorem says more precisely is that there exists an integer k such that $B_1, \ldots, B_k$ is a maximal collection of admissible balls such that each ball bounds a region containing a prime link (after choosing a connecting arc between the intersection points on the decomposing sphere). And moreover, the unordered list of these prime links is unique. For knots it is the case that the unordered list of prime factors determines the knot, but this is not the case for links as is shown in Example 6.

While there has been much attention given to the tabulation of prime links in S^3 up to this equivalence, the composite links remain largely unstudied. It is the main purpose of this note to present an orderly algorithm for computing the composite knots from the tables of prime knots and to discuss the obstructions to tabulating composite links. The symmetry information of the prime factors is an essential ingredient. One obstruction in the literature has been lack of this symmetry information. The symmetry data for all prime knots and links through 8 crossings has been tabulated by Cantarella, et al [Ber12]. Using this data we will tabulate the composite knots whose prime factor's crossing numbers sum to at most 12 crossings including the symmetry data. Note that this is not necessarily the crossing number of the composites as it is still unknown whether or not crossing numbers is additive with respect to connected sum.

Example 6. Consider taking the connected sum of a Hopf link, a right handed trefoil, and a left handed trefoil. One way to take the connected sum is to attach the trefoils first to produce a square knot and then add on the Hopf link (see Figure 1.3). This produces a 2-component link with an unknotted component. On the other hand we could attach one trefoil to each component of the Hopf link producing a 2-component link where both components are trefoils. These two links are clearly not isotopic, but have the same "prime factorization."

1.2 JSJ-Decompositions

We now describe the JSJ-decomposition of a 3-manifold with torus boundary (though we will only be interested in the knot complements in S^3) following the presentation of Neumann and Swarup [WN97]. This decomposition was first described by and named for Jaco and Shalen [JS76] as well as independently by Johannson [Joh79].

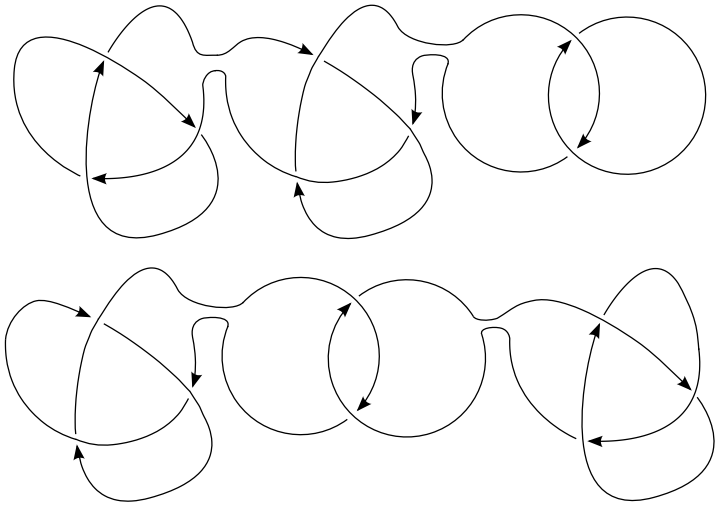

Figure 1.3: The two composite links of Example 6. These two links have the same unordered list of prime factors, but are not isotopic as the first has an unknot component while the second does not.

The notions of prime and composite knots discussed in the last section are based on sphere decompositions of S^3, and while this matches conceptually with connected sums sphere decompositions are technically frustrating. This is mainly because there are isotopically distinct embeddings of n 2-spheres in S^3. The JSJ-decomposition is more attractive from this perspective as it carries a uniqueness statement which will drive the combinatorial viewpoint of composite knots presented later.

Definition 7. Let M be a 3-manifold with boundary and N a 2-dimensional closed submanifold of M. We say that N is **boundary parallel** if it is isotopic to a boundary component of M. A **compressing disk** for N is an embedded disk in M with boundary in N which represents a non-trivial element in the first homology of N. If there are no compressing disks for N then N is called **incompressible**. We say that M is **simple** if

every incompressible torus in M is boundary-parallel. A torus embedded in M is **essential** if it is incompressible and not boundary-parallel.

As we will see, simple 3-manifolds have a trivial JSJ-decomposition. For the remainder of this section we will assume that M is not simple.

Definition 8. An essential torus S will be called **canonical** if any other properly embedded essential torus T can be isotoped to be disjoint from S. Take a disjoint collection $\{S_1, \ldots, S_s\}$ of canonical tori in M such that

- no two of the S_i are parallel;
- the collection is maximal among disjoint collections of canonical tori with no two parallel. A maximal system exists because of the Kneser-Haken finiteness theorem [**?**].

Definition 9. The collection $\{M, S_1, \ldots, S_s\}$ will be called a **JSJ-decomposition** of M. The collection of tori $\{S_1, \ldots, S_s\}$ will be called a JSJ-system.

Example 10. Figure 1.4 shows the JSJ-decomposition for the complement of a composite knot whose prime factors are a trefoil, a figure 8 knot and the Whitehead double of a figure 8 knot. This figure is borrowed from Budney [Bud06].

Lemma 11. *Let $S_1, \ldots, S_k$ be pairwise disjoint and pairwise non-parallel canonical tori in M. Then any incompressible torus T in M can be isotoped to be disjoint from $S_1 \cup \ldots \cup S_k$. Moreover, if T is not parallel to any S_i then the final position of T in $M \setminus (S_1 \cup \ldots \cup S_k)$ is determined up to isotopy.*

By assumption we can isotope T off each S_i individually. Writing $T = S_0$, the lemma is thus a special case of the stronger:

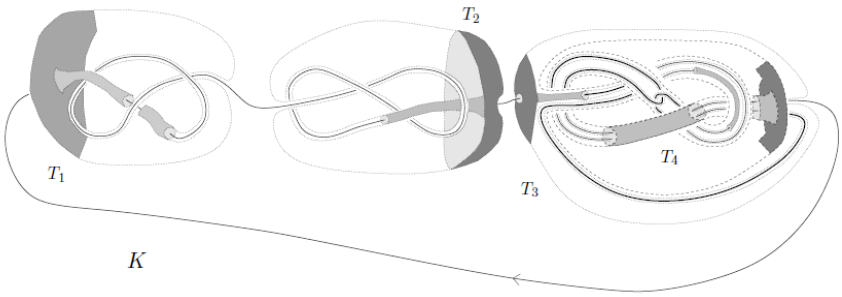

Figure 1.4: The JSJ-decomposition described in Example 10.

Lemma 12. *Suppose* $\{S_0, S_1, \ldots, S_k\}$ *are incompressible surfaces in an irreducible manifold* M *such that each pair can be isotoped to be disjoint. Then they can be isotoped to be pairwise disjoint and the resulting embedded surface* $S_0 \cup \ldots \cup S_k$ *in* M *is determined up to isotopy.*

The proof of Lemma 12 can be found in Nuemann and Swarup [WN97]. The JSJ-decomposition of a composite knot complement will appear again in Chapter 6.

Chapter 2

The Intrinsic Symmetry Group

As we will describe below following the presentation in [Ber12], the group $\mathrm{MCG}(S^3) \times \mathrm{MCG}(L)$ was first studied by Whitten in 1969 [WCW69], following ideas of Fox. The mapping class group of a manifold M is defined to be the automorphism group of M modulo the subgroup of automorphisms which are isotopic to the identity. They denoted the group $\mathrm{MCG}(S^3) \times \mathrm{MCG}(L)$ by $\Gamma(L)$ or Γ_μ, where μ is the number of components of L. When $\mu = 1$ we will refer to this group as simply Γ. We can write this group as a semidirect product of $\mathbb{Z}_2$ groups encoding the orientation of each component of the link L with the permutation group S_μ exchanging components of L (cf. Definition 14), finally crossed with another $\mathbb{Z}_2$ recording the orientation of S^3:

$$\Gamma(L) = \Gamma_\mu = \mathbb{Z}_2 \times (\mathbb{Z}_2^\mu \rtimes S_\mu).$$

It is clear that an element $\gamma = (\epsilon_0, \epsilon_1, \ldots, \epsilon_\mu, p) \in \Gamma(L)$ acts on L to produce a new link L^γ. If $\epsilon_0 = +1$, then L^γ and L are the same as sets (but the components of L have been renumbered and reoriented), while if $\epsilon_0 = -1$ the new link L^γ is the mirror image of L (again with renumbering and reorientation).

Definition 13. We define the **symmetry subgroup** $\Sigma(L)$ by $\gamma \in \Sigma(L)$ if and only if there is an isotopy from L to L^γ preserving component numbering and orientation.

For knots, $\Sigma(L) < \Gamma_1 = \mathbb{Z}_2 \times \mathbb{Z}_2$. Here the five subgroups of $\mathbb{Z}_2 \times \mathbb{Z}_2$ correspond to the standard descriptions of the possible symmetries for a knot, as shown in Table 2.1.

Symmetry subgroup of Γ_1	Name	Example(s)
$\{(1,1)\}$	No Symmetry	$9_{32}, 9_{33}$
$\{(1,1),(-1,1)\}$	(+) Amphichiral Symmetry	12_{427}
$\{(1,1),(1,-1)\}$	Invertible Symmetry	3_1
$\{(1,1),(-1,-1)\}$	(-) Amphichiral Symmetry	8_{17}
Γ_1	Full Symmetry	4_1

Table 2.1: The five standard symmetry types for knots correspond to the five subgroups of the Whitten group Γ_1.

For links, the situation is more interesting, as the group $\Gamma(L)$ is more complicated. In the case of two-component links, the group $\Gamma_2 = \mathbb{Z}_2 \times (\mathbb{Z}_2 \times \mathbb{Z}_2 \rtimes S_2)$ is a nonabelian 16 element group isomorphic to $\mathbb{Z}_2 \times D_4$. The various subgroups of Γ_2 do not all have standard names, but we will call a link *purely invertible* if $(1, -1, \ldots, -1, e) \in \Sigma(L)$, and say that components (i, j) have a *pure exchange* symmetry if $(1, 1, \ldots, 1, (ij)) \in \Sigma(L)$.

Increasing the number of components in a link greatly increases the number of possible types of symmetry. Table 2.2 lists the number of subgroups of Γ_μ; each different subgroup represents a different intrinsic symmetry group that a μ-component link might have. We note that if $\Sigma(L)$ is the symmetry subgroup of link L, then the symmetry subgroup of L^γ is the conjugate subgroup $\Sigma(L^\gamma) = \gamma\Sigma(L)\gamma^{-1}$. Therefore, it suffices to only examine the number of mutually nonconjugate subgroups of Γ_μ in order to specify all of the different intrinsic symmetry groups. Table 2.2 also lists the number of conjugacy classes of subgroups of Γ_μ, and the number of these which appear for prime links of 8 or fewer crossings.

μ	$\lvert\Gamma_\mu\rvert$	# subgroups	# subgroups (up to conjugacy)	nonconjugate ones for ≤ 8 crossings
1	4	5	5	3
2	16	35	27	5
3	96	420	131	7
4	768	9417	994	3
5	7680	270131	6382	0

Table 2.2: The number of subgroups of Γ_μ; each one represents a different intrinsic symmetry group possible for a μ-component link. The number of nonconjugate symmetries (the fourth column) is given by the number of conjugacy classes of subgroups. This article computes the symmetry group for all prime links of 8 or fewer crossings; the last column summarizes our results.

We now give the details of our construction of the Whitten group $\Gamma(L)$ and the symmetry group $\Sigma(L)$. Consider operations on an oriented, labeled link L with μ components. We may reverse the orientation of any of the components of L or permute the components of L by any element of the permutation group S_μ. However, these operations must interact with each other as well: if we reverse component 3 and exchange components 3 and 5, we must decide whether the orientation is reversed before or after the permutation. Further, we can reverse the orientation on the ambient S^3 as well, a process which is clearly unaffected by the permutation. To formalize our choices, we follow [WCW69] to introduce the Whitten group of a μ-component link.

Definition 14. Consider the homomorphism given by

$$\omega : S_\mu \longmapsto \ \mathrm{Aut}(\mathbf{Z}_2^{\mu+1}), \qquad p \longmapsto \omega(p)$$

where $\omega(p)$ is defined as

$$\omega(p)(\epsilon_0, \epsilon_1, \epsilon_2 ... \epsilon_\mu) = (\epsilon_0, \epsilon_{p(1)}, \epsilon_{p(2)} ... \epsilon_{p(\mu)}).$$

For $\gamma = (\epsilon_0, \epsilon_1, ... \epsilon_\mu, p)$, and $\gamma' = (\epsilon'_0, \epsilon'_1, ... \epsilon'_\mu, q) \in \mathbf{Z}_2^{\mu+1} \rtimes_\omega S_\mu$, we define the *Whitten group* Γ_μ as the semidirect product $\Gamma_\mu = \mathbf{Z}_2^{\mu+1} \rtimes_\omega S_\mu$ with the group operation

$$\begin{aligned} \gamma * \gamma' &= (\epsilon_0, \epsilon_1, \epsilon_2 ... \epsilon_\mu, p) * (\epsilon'_0, \epsilon'_1, \epsilon'_2 ... \epsilon'_\mu, q) \\ &= ((\epsilon_0, \epsilon_1, \epsilon_2 ... \epsilon_\mu) \cdot \omega(p)(\epsilon'_0, \epsilon'_1, \epsilon'_2 ... \epsilon'_\mu), qp) \\ &= (\epsilon_0 \epsilon'_0, \epsilon_1 \epsilon'_{p(1)}, \epsilon_2 \epsilon'_{p(2)} ... \epsilon_\mu \epsilon'_{p(\mu)}, qp) \end{aligned}$$

We will also use the notation $\Gamma(L)$ to refer to the **Whitten group** Γ_μ.

2.1 Link Operations

Given a link L consisting of μ oriented knots in S^3, we may order the knots and write

$$L = K_1 \cup K_2 \cup \cdots \cup K_\mu.$$

Consider the following operations on L:

1. Permuting the K_i.
2. Reversing the orientation of any set of K_i's
3. Reversing the orientation on S^3 (mirroring L).

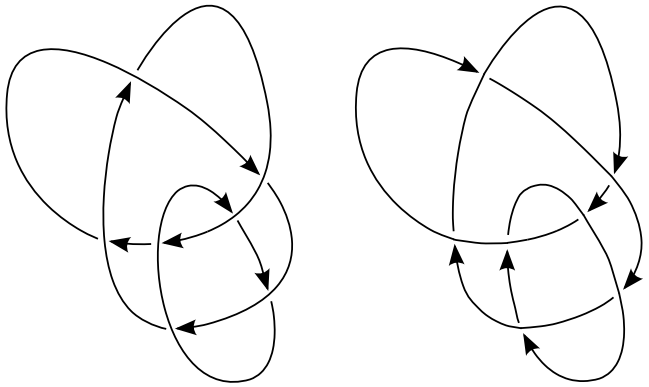

Figure 2.1: A link and its mirror image. The element $(-1, 1, 1, e)$ relates these two diagrams.

Let γ be a combination of any of the moves (1), (2), or (3). We think of $\gamma = (\epsilon_0, \epsilon_1, ...\epsilon_\mu, p)$ as an element of the set $\mathbf{Z}_2^{\mu+1} \times S_\mu$ in the following way. Let

$$\epsilon_0 = \begin{cases} -1, & \text{if } \gamma \text{ mirrors } L \\ +1, & \text{if } \gamma \text{ does not mirror } L \end{cases}$$

and

$$\epsilon_i = \begin{cases} -1, & \text{if } \gamma \text{ reverses the orientation of } K_{p(i)} \\ +1, & \text{if } \gamma \text{ does not reverse the orientation of } K_{p(i)} \end{cases}$$

Lastly, let $p \in S_\mu$ be the permutation of the K_i associated to γ. To be explicitly clear, permutation p permutes the labels of the components; the component originally labeled i will be labeled $p(i)$ after the action of γ.

For each element, γ in $\mathbf{Z}_2^{\mu+1} \times S_\mu$, we define

$$L^\gamma = \gamma(L) = \epsilon_1 K_{p(1)}^{(*)} \cup \epsilon_2 K_{p(2)}^{(*)} \cup \cdots \cup \epsilon_\mu K_{p(\mu)}^{(*)} = \bigcup_{i=1}^{\mu} \epsilon_i K_{p(i)}^{(*)} \tag{2.1}$$

where $-K_i$ is K_i with orientation reversed, K_i^* is the mirror image of K_i and the $(*)$ appears above if and only if $\epsilon_0 = -1$. Note that the ith component of $\gamma(L)$ is $\epsilon_i K_{p(i)}^{(*)}$ the possibly reversed or mirrored $p(i)$th component of L. Since we are applying ϵ_i instead of $\epsilon_{p(i)}$ to $K_{p(i)}$ we are taking the convention of first permuting and then reversing the appropriate components.

Example 15. Let $L = K_1 \cup K_2 \cup K_3$ and $\gamma = (1, 1, -1, 1, (123))$. Then, $\gamma(L) = K_2 \cup -K_3 \cup K_1$.

Example 16. Let $L = K_1 \cup K_2 \cup K_3 \cup K_4$ and $\gamma = (-1, 1, 1, -1, -1, (14)(23))$. Then, $\gamma(L) = (K_4^* \cup K_3^* \cup -K_2^* \cup -K_1^*)$. Since we have reversed the orientation on S^3, note that $\gamma(L)$ will be the mirror image of L as well.

We now confirm that this operation defines a group action of the Whitten group $\Gamma(L)$ on the set of links obtained from L by such transformations.

Proposition 17. *The Whitten group* $\Gamma(L)$ *is isomorphic to the group* $\mathrm{MCG}(S^3) \times \mathrm{MCG}(L)$.

Proof. We know that L is a disjoint union of μ copies of S^1 denoted $L = K_1 \sqcup \cdots \sqcup K_\mu$. Further, the mapping class groups of S^1 and S^3 are both $\mathbb{Z}_2$ [Cer68], where the elements ± 1 correspond to orientation preserving and reversing diffeomorphisms of S^1 and S^3. In general, the mapping class group of μ disjoint copies of a space is the semidirect product of the individual mapping class groups with the permutation group S_μ. This means that $\mathrm{MCG}(L) = (\mathbb{Z}_2)^\mu \rtimes S_\mu$ and the Whitten group $\Gamma(L)$ has a bijective map to $\mathrm{MCG}(S^3) \times \mathrm{MCG}(L)$.

It remains to show that the group operation $*$ in the Whitten group maps to the group operation (composition of maps) in $\mathrm{MCG}(S^3) \times \mathrm{MCG}(L)$. To do so, we introduce some notation. Let $\gamma = (\epsilon_0, \epsilon_1, ...\epsilon_\mu, p)$ and $\gamma' = (\epsilon_0', \epsilon_1', ...\epsilon_\mu', q)$. We must show

$$L^{\gamma * \gamma'} = (\gamma \circ \gamma')(L) = \gamma(\gamma'(L))$$

where $\gamma * \gamma'$ is the operation of the Whitten Group, Γ_μ.

Then,

$$\gamma'(L) = \gamma'\left(\bigcup_{i=1}^{\mu} K_i\right) = \bigcup_{i=1}^{\mu} \epsilon_i' K_{q(i)} = \bigcup_{i=1}^{\mu} X_i,$$

where X_i denotes the i-th component $\epsilon_i' K_{q(i)}$ of $\gamma'(L)$.

$$\gamma(\gamma'(L)) = \gamma\left(\bigcup_{i=1}^{\mu} \epsilon_i' K_{q(i)}\right) = \gamma\left(\bigcup_{i=1}^{\mu} X_i\right) = \bigcup_{j=1}^{\mu} \epsilon_i X_{p(i)}.$$

Note that $X_{p(i)} = \epsilon'_{p(i)} K_{q(p(i))}$, which implies

$$\gamma(\gamma'(L)) = \bigcup_{i=1}^{\mu} \epsilon_i (\epsilon'_{p(i)} K_{q(p(i))}).$$

Now, $\gamma * \gamma' = (\epsilon_0\epsilon_0', \epsilon_1\epsilon'_{p(1)}, \epsilon_2\epsilon'_{p(2)}, ..., \epsilon_\mu\epsilon'_{p(\mu)}, qp)$ and acts on L as

$$\begin{aligned} L^{\gamma*\gamma'} &= \epsilon_1\epsilon'_{p(1)} K_{qp(1)} \cup \epsilon_2\epsilon'_{p(2)} K_{qp(2)} \cup \ldots \cup \epsilon_\mu\epsilon'_{p(\mu)} K_{qp(\mu)} \\ L^{\gamma*\gamma'} &= \bigcup_{i=1}^{\mu} \epsilon_{p(i)} (\epsilon_i' K_{qp(i)}) = \gamma(\gamma'(L)) \end{aligned}$$

We have dropped the notation for mirroring throughout the proof, because the two links clearly agree in this regard. The element $\gamma * \gamma'$ preserves the orientation of S^3 if and only if $\epsilon_0\epsilon_0' = 1$, i.e., if either both or neither of γ and γ' mirror L. □

Definition 18. We say that two μ-component links in S^3 have the same **base type** if they are related by an element of $\Gamma(\mu)$.

The standard knot and link tables ([CL11], [BN11])only consider link equivalence up to base type. It is likely that this is because many of the standard link invariants such as the fundamental group of the complement are only defined up to base type.

We can now define the subgroup of $\Gamma(L)$ which corresponds to the symmetries of the link L.

Definition 19. Given a link, L and $\gamma \in \Gamma(L)$, we say that L *admits* γ when there exists an isotopy taking each component of L to the corresponding component of L^γ which respects the orientations of the components. We define as the **Whitten symmetry group** of L,

$$\Sigma(L) := \{\gamma \in \Gamma(L) |\ L \text{ admits } \gamma\}.$$

The Whitten symmetry group $\Sigma(L)$ is a subgroup of Γ_μ, and its left cosets represent the different isotopy classes of links L^γ among all symmetries γ. By counting the number of cosets, we determine the number of (labeled, oriented) isotopy classes of a particular prime link.

2.2 Examples of Symmetry Groups of Prime Links

Next, we provide a few examples of symmetry subgroups. Recall that the first Whitten group $\Gamma_1 = \mathbb{Z}_2 \times \mathbb{Z}_2$ has order four and that $\Gamma_2 = \mathbb{Z}_2 \times (\mathbb{Z}_2 \times \mathbb{Z}_2 \rtimes S_2)$ is a nonabelian 16 element group.

Example 20. Let $L = 4_1$, the figure eight knot. Since $L \sim -L \sim L^* \sim -L^*$, we have $\Sigma(4_1) = \Gamma_1$, so the figure eight knot has *full symmetry*. There is only one coset of $\Sigma(4_1)$ and hence only one isotopy class of 4_1 knots.

Example 21. Let $L = 3_1$, a trefoil knot. It is well known that $L \sim -L$ and $L^* \sim -L^*$, but $L \nsim L^*$, so we have $\Sigma(3_1) = \{(1, 1, id), (1, -1, e)\}$. This means that the two cosets of $\Sigma(3_1)$ are $\{(1, 1, id), (1, -1, id)\}$ and $\{(-1, -1, id), (-1, 1, id)\}$, and there are two isotopy classes of 3_1 knots. A trefoil knot is thus *invertible*.

Example 22. Let $L = 7_5^2$, whose components are an unknot K_1 and a trefoil K_2. Since the components K_1 and K_2 are of different knot types, we conclude that no symmetry in $\Sigma(7_5^2)$ can contain the permutation (12). Since $K_2 \nsim K_2^*$, we cannot mirror L, i.e., the first entry of $\gamma \in \Sigma(7_5^2)$ cannot equal -1. The linking number of L is nonzero, so we can rule out the symmetries $(1, -1, 1, e)$ and $(1, 1, -1, e)$. Last, L is purely invertible, meaning isotopic to $-L = -K_1 \cup -K_2$. Thus, $\Sigma(L)$ is the two element group $\Sigma_{2,1} = \{(1, 1, 1, e), (1, -1, -1, e)\}$. There are 8 cosets of this two element group in the 16 element group Γ_2, so there are 8 isotopy classes of 7_5^2 links.

We now prove

Proposition 23. *The Whitten symmetry group* $\Sigma(L)$ *is the image of* $\mathrm{Sym}(L)$ *under the map* $\pi : \mathrm{Sym}(L) = \mathrm{MCG}(S^3, L) \to \mathrm{MCG}(S^3) \times \mathrm{MCG}(L) = \Gamma(L)$.

Proof. Given a map $f : S^3 \to S^3 \in \mathrm{MCG}(S^3, L)$, we see that if f is orientation-preserving on S^3, then it is homotopic to the identity on S^3 since $\mathrm{MCG}(S^3) = \mathbb{Z}_2$. This homotopy yields an ambient isotopy between L and $f(L)$, proving that $f|_L = \pi(f) \in \Sigma(L)$. If f is orientation-reversing on S^3, it is homotopic to a standard reflection r. Composing the homotopy with r provides an ambient isotopy between L and $r(f(L))$, proving that $\pi(f) \in \Sigma(L)$. This shows $\pi(\mathrm{Sym}(L)) \subset \Sigma(L)$.

Now suppose $g \in \Sigma(L)$. The isotopy from L to $g(L)$ generates an orientation-preserving (since it is homotopic to the identity) diffeomorphism $f : S^3 \to S^3$ which either fixes L or takes L to rL. In the first case, $f \in \mathrm{Sym}(L)$. In the second, the map $rf \in \mathrm{Sym}(L)$. □

Chapter 3

Link Diagrams and PD-Codes

Note that elements in $\Sigma(L)$ will always act trivially on a link. This is problematic for the purpose of computing symmetries of composites as it will be useful for us to distinguish a link L from γL even if $\gamma \in \Sigma(L)$. To remedy this issuew we will consider planar diagrams instead of knots. A planar diagram code (PD-code) is a collection of combinatorial data that encodes the information of a link diagram [BN11]. Our first goal in this section is to make this statement precise.

3.1 Link Diagrams

Definition 24. Let S be a closed, oriented, not necessarily connected, surface. A **link diagram** on S is an oriented immersion of $d : \sqcup_n S^1 \to S$ with only finitely many transverse double self intersections and no other self intersections. We take the $\sqcup_n S^1$ to be ordered. Call the self intersections of the immersion the vertices and the arcs between vertices will be called edges. A diagram also includes a labeling of the edges by pairs (i, j) where i is the index of the S^1 which contains the edge and j gives a cyclic ordering of the arcs. In the case

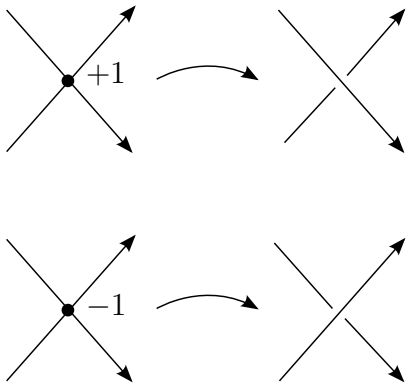

Figure 3.1: Over and under crossings. Here the orientation is taken to be the standard orientation of the plane of the page.

of a knot we will omit the first element in the pair. We will often use the notation for knots and only label edges with integers to avoid overcrowding figures. In addition, the vertices will be called crossings and are equipped with a coloring by the set $\{1, -1\}$. Two diagrams are equivalent if there is an isotopy of S which brings one diagram to the other respecting the labeling. We will denote the set of equivalence classes of diagrams by $\mathbb{D}$.

Each crossing of a diagram involves four edges. Edges that are oriented toward the vertex will be called incoming edges and the others will be outgoing. Each pair of non-adjacent edges will be referred to as either the over edges or the under edges as determined by the following criterion. If the counter-clockwise ordered pair of outgoing tangents at the vertex (T_1, T_2) agrees with the orientation of S, then the edge corresponding to T_1 is the over edge if the sign of the vertex is positive and the under edge if the sign of the vertex is negative. This is illustrated in Figure 3.1.

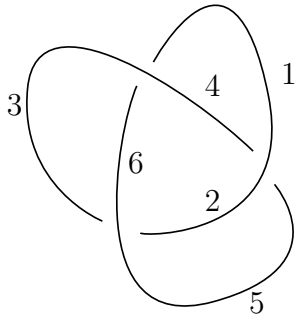

$\{[+4,-2,-5,+1],[+2,-6,-3,+5],$
$[+6,-4,-1,+3]\}$

Figure 3.2: A diagram for 3_1 and its PD-code. The labels are only single integers here as there is only one component

3.2 PD-codes

Definition 25. Given a link diagram we generate the set of quadruples of the **PD-code** representing this diagram by the following procedure. For each crossing we include the quadruple of arc labels involved beginning with the incoming under crossing and proceeding around the crossing in the counter-clockwise direction (see Figures 3.2 and 3.3). We give a positive sign to incoming edges and a negative sign to outgoing edges.

Definition 26. Let $\overline{\mathbb{PD}}$ be the set of collections of quadruples of the labels

$$\{(1,1),\ldots,(1,n_1),\ldots,(\mu,1),\ldots,(\mu,n_\mu)\}$$

satisfying the following properties.

1. Each edge label appears exactly twice, once with a positive sign and once with a negative sign on the second coordinate.

2. Each quadruple contains two positive edges and two negative edges and begins with a positive label.

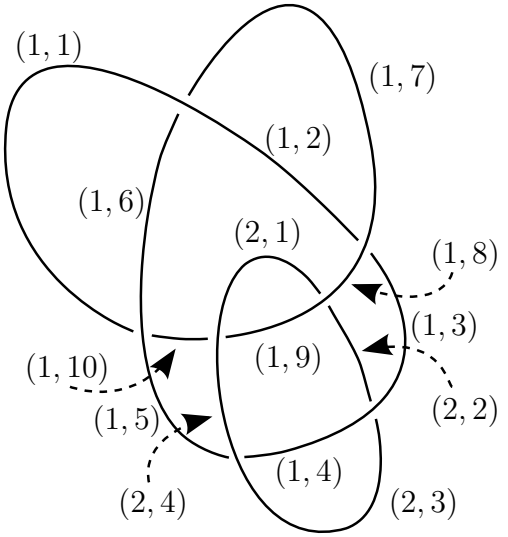

$\{[(1,+6),(1,-2),(1,-7),(1,+1)],$
$[(1,+2),(1,-8),(1,-3),(1,+7)],$
$[(2,+1),(1,-9),(2,-2),(1,+8)],$
$[(1,+9),(2,-1),(1,-10),(2,+4)],$
$[(1,+10),(1,-6),(1,-1),(1,+5)],$
$[(2,+2),(1,-4),(2,-3),(1,+3)],$
$[(1,+4),(2,-4),(1,-5),(2,+3)]\}$

Figure 3.3: A link diagram and the corresponding PD-code.

3. The second coordinate of non-adjacent edge labels in each quadruple are consecutive modulo the number of arcs in those edges component.

4. Non-adjacent edge labels have opposite sign and the lesser edge label is always positive.

It is natural to ask what information is contained in a PD code. Can a link diagram be reconstructed from a PD code? To answer this question we will first step back and study how surfaces can be constructed from 4-regular graphs with extra information.

We will use the following definition of a graph. The edge labels might seem strange, but when we apply graphs of this sort to link diagrams it will be convenient to label the edges as defined below.

Definition 27. A **graph** is an ordered pair (E, V) where E is a set of edges labeled by pairs $\{(1,1),\ldots,(1,n_1),\ldots,(\mu,1),\ldots,(\mu,n_\mu)\}$ and V is a multi-set (a set with duplicates allowed, this is to allow loops at a single vertex) of unordered lists of labels such that each edge label appears exactly twice throughout the collection of lists. The unordered lists will

be referred to as vertices and we say that an edge is incident to a vertex if it appears in the corresponding list. Let (E, V) and (E', V') be two graphs. We say that two graphs (E, V) and (E', V') are isomorphic if there is a bijection $\phi : E \to E'$ such that $\{e_1, ..., e_k\} \in V$ if and only if $\{\phi(e_1), ..., \phi(e_k)\} \in V'$.

Lemma 28. *Let (E, V) be a graph, then*

1. *If $\sigma_1 \in S_\mu$ there is a graph isomorphism from (E, V) to (E', V') where*

$$E' = \{(\sigma_1(1), 1), \ldots, (\sigma_1(1), n_1), \ldots, (\sigma_1(\mu), 1), \ldots, (\sigma_1(\mu), n_\mu)\}$$

and

$$V' = \{\{(\sigma_1(i_1), j_1), \ldots, (\sigma_1(i_k), j_k)\} : \{(i_1, j_1), \ldots, (i_k, j_k)\} \in V\}$$

2. *If $\sigma_2 \in S_{n_i}$ there is a graph isomorphism from (E, V) to (E, V') where V' is obtained from V by applying σ_2 to the second coordinate of every edge whose label appears in the appropriate section of labels. Note that the edge sets are the same in this case as the action of σ_2 on the second coordinate of the edges is a permutation of E.*

Proof. We first verify item 1. Define $\phi : E \to E'$ by $(i, j) \mapsto (\sigma_1(i), j))$. We know that ϕ is a bijection since σ_1 is a bijection. By construction we have that $\{e_1, ..., e_k\} \in V$ if and only if $\{\phi(e_1), ..., \phi(e_k)\} \in V'$.

For item 2 we note that any permutation of the edges induces a graph isomorphism with the above definition of vertex sets. □

Definition 29. Given a 4 regular graph we define a **cyclic ordering at the vertices** to be an ordering of the 4 edge ends incident a vertex v_i. We will denote the ordering at vertex v_i by $(v_i^0, v_i^1, v_i^2, v_i^3)$. Note that a single edge may be incident to the same vertex twice and thus the ordering labels need not correspond to distinct edges. We define the successor function by $s(v_i^j) = v_k^{l+1 \mod (4)}$ where v_k^l is the other appearance of the edge v_i^j.

Definition 30. Given a 4 regular graph with a cyclic ordering at the vertices we will construct the **associated cell complex**. The set of 0-cells is the vertex set and the set of 1 cells is the edge set so that the one skeleton is the graph. The 2 cells are defined to be polygons in the plane indexed by the orbits of the set $\{v_i^j\}$ under successive applications of the map s and whose edges correspond to the elements in the corresponding orbit. The 2 cells are glued to the one skeleton according to their edge labeling.

Proposition 31. *The cell complex associated to a* 4 *regular graph with a cyclic ordering at the vertices is homeomorphic to a closed smooth surface.*

Proof. Let P be the cell complex corresponding to these identifications. To see that P is homeomorphic to a closed surface we will first show that the gluing given in Definition 30 is a piece-wise linear surface. There is nothing to check at interior points of the faces. Let x be a point on edge e and let I be an open interval in e. There are exactly 2 faces, say f_1 and f_2, incident to edge e because the orbits partition the edges and each edge appears exactly twice. Each of these faces is a polygon in the plane so we may take U_{f_1} and U_{f_2} to be open balls in f_1 and f_2 which intersect the boundaries at exactly I. In P we may now construct the set $U_{f_1} \cup I \cup U_{f_2}$ which is homeomorphic to an open disk in the plane. It is left to check that there is a neighborhood of each vertex which is homeomorphic to a ball in the plane. By construction each vertex is locally incident to exactly 4 faces. In addition, near each vertex there are four distinct edges where adjacent edges in the quadruple bound a distinct triangle in the corresponding face (see Figure 3.4). Therefore, two edges either correspond to a unique triangle or they are not the boundary of any triangle. Thus, each vertex has a neighborhood which is homeomorphic to a piecewise linear disk. So, P is homeomorphic to a closed piecewise linear surface though it need not be either connected or orientable. Since we have a finite cell complex we can appeal to the classification of surfaces and assume that our surface is smooth. We will call this the surface associated to the diagram.

□

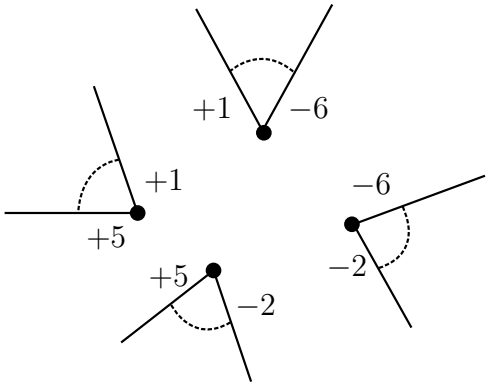

Figure 3.4: Four faces coming together at a vertex to form a disk.

Proposition 32. *Given a PD-code we can produce a well-defined link diagram.*

Proof. Given a PD code C we first produce a graph with a cyclic ordering at the vertices. Let the vertex set be the set of quadruples and the edge set be the set $\{(1,1),\ldots,(1,n_1),\ldots,(\mu,1),\ldots,(\mu,n_\mu)\}$ of labels in C (neglecting signs). An edge is incident to a vertex if its label appears in the vertices' quadruple. We get an ordering at the vertices by the order of the labels in each quadruple. Thus, by Proposition 31 we can produce a surface S with a cell decomposition corresponding to C. We will now use the remaining data in C to define a link diagram on S using the 1 skeleton of the cell decomposition. Beginning with edge $(1,1)$ we traverse the 1 skeleton by choosing the non-adjacent edge according to the ordering at each vertex. Property 4 of Definition 26 implies that the resulting cycle can be given an orientation by orienting each edge from the negative label to the positive. Thus, we have an oriented immersion from S^1 into S. We repeat this process until every edge is contained in a cycle thus producing an oriented immersion $d : \sqcup_n S^1 \to S$ where the $\sqcup_n S^1$ are ordered. We color each vertex by $\{1,-1\}$ according to Figure 3.1 with the convention that the first label of each quadruple is the incoming under crossing. □

It is important to note that the map of Proposition 32 and the algorithm for computing a PD-code from a diagram are not inverses. For example, if one placed the standard diagram for the trefoil inside an embedded disk on the torus one would obtain the same PD-code as the standard diagram for the trefoil on a sphere. In this case the map of Proposition 32 will produce the diagram of the trefoil on the sphere (cf. example).

Definition 33. The **surface associated to a PD-code** C is the closed smooth surface associated to the 4 regular graph with an ordering at the vertices underlying C (cf. Proposition 32). We say the PD-code is **connected** if the associated surface is connected.

Proposition 32 and Proposition 31 imply that the surface associated to a PD-code is well-defined.

Definition 34. Define $\mathbb{PD}$ to be the subset of the set of all PD-codes $\overline{\mathbb{PD}}$ (cf. Definition 26) whose associated surfaces are 2-spheres.

Proposition 35. $\mathbb{PD}$ *is in bijection with the set of link diagrams on* 2*-spheres (cf. Definition 24).*

Proof. Definition 25 gives a map from link diagrams to PD-codes and Proposition 32 gives a map from PD-codes to link diagrams. We must show that these maps are inverses when restricted to link diagrams on the 2-sphere and the set of PD-codes $\mathbb{PD}$ (cf. Definition 34).

First, consider the image C of a link diagram D under the map of Definition 25. The link diagram D on the 2-sphere gives a natural cell decomposition. The 0-cells are the self-intersection, the 1-cells are the arcs, and the 2-cells are polygons which form the complement of the diagram. It is clear that the map of Proposition 32 recovers a cell decomposition with the same number of 0-cells and 1-cells and by the definition of the successor map the 2-cells are polygons in bijection with the decomposition given by the link diagram. Moreover, the gluing map given in Proposition 32 ensures that the 2-cell adjacency relations in the link

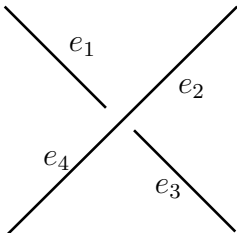

Figure 3.5: The edges e_i.

diagram as well as the associated surface agree. Therefore, the 1-skeleton of D must be isotopic to the 1-skeleton of the diagram reconstructed from C.

Now consider the image D of a PD-code C under the map given in Proposition 32. The arc labels of D are given by the labels of C as is the over/under crossing information. We again have that the adjacency relations of the 2-cells are preserved. Therefore if we read the PD-code as in Definition 25 from D we recover C. □

Definition 36. Let the **Euler characteristic of a PD-code** be the Euler characteristic of the corresponding polyhedron. We define the genus of a diagram to be $g = \sum_i g_i$ where the sum is over the connected components of the associated surface.

Theorem 37. *The Euler characteristic of an n crossing PD-code is given by $N(s) - n$ where $N(s)$ is the number of orbits of s on the set of edge labels.*

Proof. The polyhedron corresponding to D has n vertices, $2n$ edges, and $N(s)$ faces. Computing the Euler characteristic we see that $n - 2n + N(s) = N(s) - n$. □

Example 38. Consider the PD-code $\{[+4, -2, -5, +1], [+2, -6, -3, +5], [+6, -4, -1, +3]\}$ from Figure 3.2. There are 3 vertices and 6 edges and to find the faces we first write out the map s.

$s(+4) = +2;$	$s(+2) = +6;$	$s(+6) = +4$
$s(-2) = +5;$	$s(-6) = +3;$	$s(-4) = +1$
$s(-5) = -1;$	$s(-3) = -5;$	$s(-1) = -3$
$s(+1) = -4;$	$s(+5) = -2;$	$s(+3) = -6$

Table 3.1: The successor map from Example 38

Computing the orbits of this map on the set of edge labels gives that the set of faces is $\{(+1,-4),(-1,-3,-5),(-2,+5),(+2,+6,+4),(-6,+3)\}$. The Euler characteristic of the corresponding surface is 2 and so this is a genus 0 PD-code.

Proposition 39. *Given a link diagram on an oriented surface S there is a well-defined isotopy class of links in the 3-manifold $S \times [-1,1]$ that is naturally associated to S.*

Proof. Given a particular link diagram D we produce a link in $S \times [-1,1]$ by the following procedure. On each connected component of S choose disjoint neighborhoods V_i of every vertex with each neighborhood diffeomorphic to $D^2 \times [-1,1]$. Let $\{f_i\}$ be a collection of non-negative bump functions indexed by the vertices and with f_i supported in V_i. We define the push off of our diagram to be D outside of $\cup V_i$ and in each V_i we replace D with $(d(x), \epsilon f)$ where $\epsilon \in \{-1,1\}$ is chosen so that the result agrees with Figure 3.1.

Since any link diagram equivalent to D can be isotoped on S to coincide with D we can associate a link in $S \times [-1,1]$ to an equivalence class of link diagrams (cf. Definition 24). We denote the resulting link by $L(D)$. □

Note that many different link diagram can produce the same link. For example, we could relabel the diagram which would give a new PD-code, but correspond to the same link in $S \times [-1,1]$.

Lemma 40. *The isotopy class of the pair $(\sqcup S^1, S \times [-1,1])$ produced is independent of the choice of the functions f_i.*

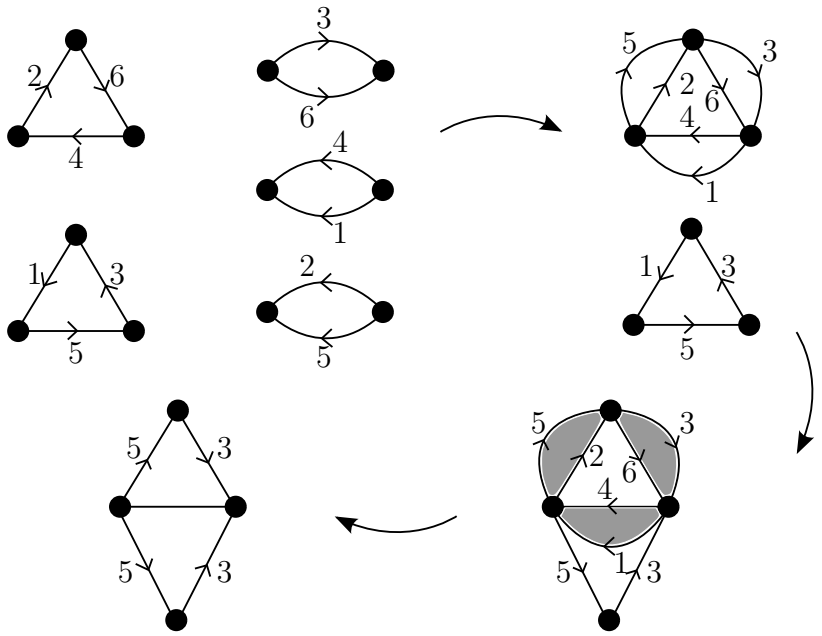

Figure 3.6: The faces and resulting polyhedron from Example 38.
The shaded disks disappear in the last step to produce an identification for a 2-sphere.

Proof. Any two bump functions f_i and f_i' on V_i are related by the straight line isotopy $h(t,x) := tf_i + (1-t)f_i'$. The push off is defined uniquely by the choice of the functions f_i and f_i' and so the resulting pairs are isotopic. □

Definition 41. Consider an ordered list of knot PD-codes (C_1, C_2) where the first has n_1 arcs and the second has n_2 arcs. We define the **connected sum of the PD-codes** to be the PD-code obtained by the following procedure (cf. Figure 3.7).

1. First add n_2 to each label of C_1 except label -1.

2. Now change the -1 to a $-n_2 + 1$ in the quadruple of C_2 which also contains $+n_2$.

3. Lastly concatenate C_1 and C_2.

The notion of studying links via their PD-codes seems to be a powerful idea. We have restricted our attention to the PD-codes whose associated surfaces are spheres because these

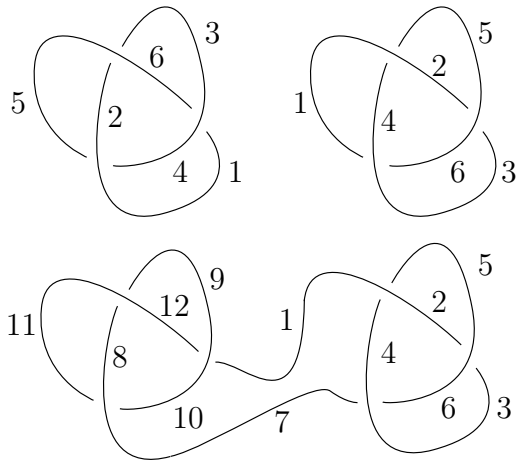

Figure 3.7: The connected sum of two diagrams.

correspond to classical knots. However, it is plausible that relaxing this condition and studying the collection of PD-codes whose associated surfaces are orientable, but of arbitrary genus should lead to the theory of virtual links [Kau11].

It would also be interesting to study knots in arbitrary 3-manifolds from the perspective of PD-codes. It should be possible to develop a combinatorial theory of knots in 3-manifolds by studying knot diagrams on middle surfaces of Morse decompositions.

Chapter 4

The Action of Γ_μ on PD-codes

The action of Γ_μ on links was discussed in chapter 2 and we will now discuss the corresponding action of Γ_μ on PD-codes.

Definition 42. Consider an element $\gamma = (\epsilon_0, \epsilon_1, \ldots, \epsilon_\mu, p) \in \Gamma_\mu$. We define an action of γ on the labels of a PD-code by the following ordered operations:

1. First, we apply p to the first component of each label.

2. If $\epsilon_0 = 1$ we do nothing. If $\epsilon_0 = -1$ we shift each positive crossing to the right by 1 and each negative crossing to the left by 1.

3. If $\epsilon_i = 1$ we do nothing. If $\epsilon_i = -1$ we first apply the permutation

$$(1)(2 \;\; n_1)(3 \;\; n_1 - 1)\ldots(\frac{n+2}{2} - 1 \;\; \frac{n+2}{2} + 1)(\frac{n_1+2}{2})$$

to the second component of the labels whose first component label is i, ignoring signs, then shift each quadruple to the right (or left) by 2 if the ith component is the under crossing, and finally switch the sign on the second component of every label with first component i.

It is clear that the action of these elements produces a set of quadruples, but we will now show that in fact there is a well-defined action on PD-codes.

Proposition 43. *The previous definition gives a well-defined action of* Γ_μ *on PD-codes. Moreover, the action corresponds to the action of* Γ_μ *on the underlying links.*

Proof. We must first show that the resulting collection of labels satisfies properties $1-4$ of Definition 26 and thus produces a valid PD-code. Property 1 persists as the only change to the sign of a label changes the sign of all labels, thus there are still exactly one positive label and one negative label. Property 2 persists as positive crossings have a positive second label in the first and last slots, this after shifting to the right we again begin with a positive crossing. Similarly, negative crossing have positive labels in the first two positions and so shifting to the left also gives a quadruple beginning with a positive label. Property 3 also checks out again because of the global sign change. To see that property 4 is preserved we fist note that since the sign change affects all labels we will still have that non-adjacent labels have opposite sign. However, the sign change does affect the lesser edge is positive condition. Luckily, the permutation $(1)(2\ \ n_1)(3\ \ n_1-1)\dots(\frac{n_1+2}{2})$ straightens this out.

We now turn the task of showing that we have a group action. Applying the permutations to the first coordinate of each label is the natural action of the symmetric group on the integers $\{1,\dots,\mu\}$. The information contained in a quadruple of a PD-code could be reorganized to represent an undercrossing and an overcrossing along with orientation information for both. This structure admits a $\mathbb{Z}_2 \times (\mathbb{Z}_2 \times \mathbb{Z}_2)$ action by switching the overcrossing for the undercrossing and reversing the orientations. In the case that both the undercrossing and the overcrossing appear in the same component we have the diagonal action where the second two group elements of $\mathbb{Z}_2 \times (\mathbb{Z}_2 \times \mathbb{Z}_2)$ are the same. The effect of this action on the labels in the PD-code is described by 2 and 3 of Definition 42 as seen in Figure 4.1.

□

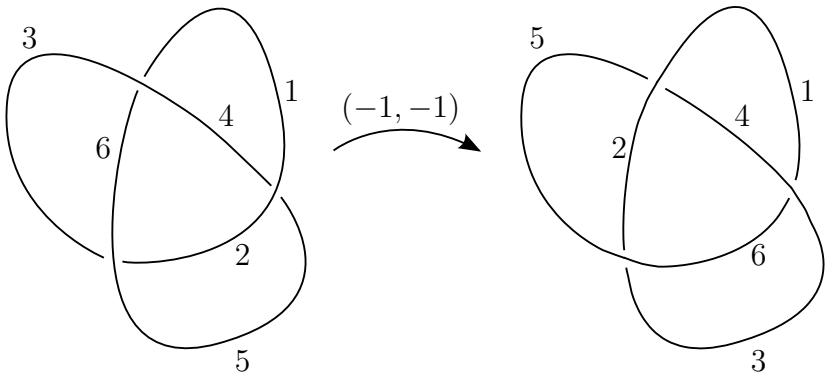

$\{[+4,-2,-5,+1],$
$[+2,-6,-3,+5],$
$[+6,-4,-1,+3]\}$

$\{[+6,+3,-1,-4],$
$[+2,+5,-3,-6],$
$[+4,+1,-5,-2]\}$

Figure 4.1: The action of $(-1,-1)$ on a diagram of the trefoil. Note that the affect on the PD-codes is as described in Definition 42.

We now address the issue of the existence of PD-codes which are fixed under the action of an element of Γ_μ. While these do exist, we will show that we can produce a list of PD-codes for knots which contain no code fixed by a non-trivial element of Γ. We will show that if we have a PD-code that is fixed by some element in Γ_μ we can add a Reidemeister 1 loop to it so that it still represents the same knot type but is not fixed by any non-identity element of Γ_μ.

Example 44. Consider the diagram and PD-code of the Hopf Link shown in Figure 4.2. The PD-code associated to this diagram is

$$\{[(1,+2),(2,-2),(1,-1),(2,+1)],[(2,+2),(1,-2),(2,-1),(1,+1)]\}.$$

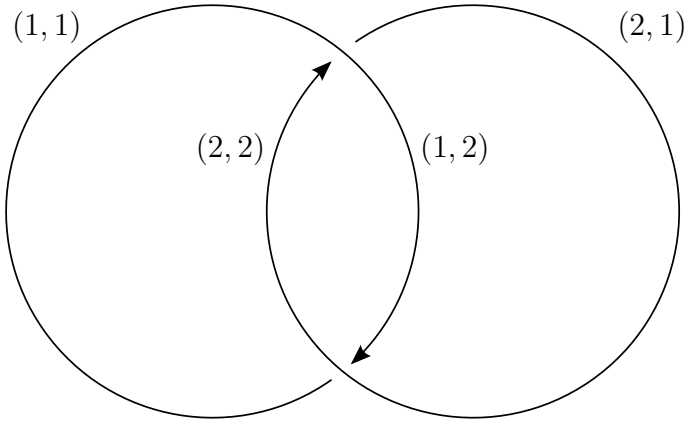

$$\{[(1,+2),(2,-2),(1,-1),(2,+1)],\\ [(2,+2),(1,-2),(2,-1),(1,+1)]\}$$

Figure 4.2: An example of a PD-code that is fixed by $(1, 1, (12))$.

If we act on this PD-code by $(1, 1, (12)) \in \Gamma_2$ the result is the PD-code

$$\{[(2,+2),(1,-2),(2,-1),(1,+1)],[(1,+2),(2,-2),(1,-1),(2,+1)]\},$$

thus the PD-code is fixed.

Lemma 45. *There is a preferred list of knot diagrams such that for each diagram in the table the corresponding PD-code is not fixed by any non-trivial element of* Γ*. Moreover, every base type is represented. We will call this list the prime knot table.*

Proof. We first observe that a Reidemeister 1 loop occurs in a diagram if and only if the corresponding PD-code contains a quadruple with two pairs with the same integer appearing as second components with opposite signs.

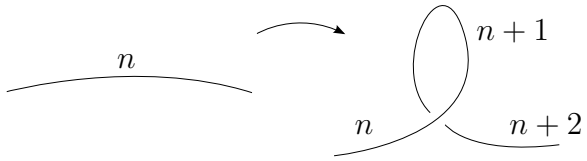

Figure 4.3: Adding a Reidemeister 1 to arc n.

Suppose we have a PD-code with exactly one Reidemeister 1 loop. Then there is a quadruple of the form $[i, -i, j, k]$,$[i, k, j, -j]$,$[i, j, -j, k]$, or $[i, j, k, -i]$. But, none of these are fixed by a shift by 1. Thus, no PD-code containing a Reidemeister 1 loop can be fixed by the action of $(-1, 1)$. Similarly, since there is no other quadruple contained both positive and negative i (or j) this PD-code cannot be fixed by $(1, -1)$.

Thus, if we have a PD-code that is fixed by some element of Γ we may modify it by first removing all Reidemeister 1 loops and then adding a single Reidemeister 1 loop. Given a table of PD-codes for knots we simply traverse the list and fix each code to produce preferred list.

The bijection of Proposition 35 ensures that we can find a PD-code for every base type.

□

Chapter 5

JSJ-Graphs and Splicing Graphs

The results in this section either appear in or are corollaries of results in the survey of Ryan Budney [Bud06].

Definition 46. Given a link $L \subset S^3$ we denote the complement $S^3 \setminus L$ by C_L.

Definition 47. We denote the standard **linking number** in S^3 by $lk(L, L')$.

Definition 48. Let $M \subset S^3$ be a 3-manifold, and let $T \subset \partial M$ be a torus. Provided C is the component of $Cl(S^3 \setminus M)$ containing T, an essential curve $c \subset T$ is called an **external (resp. internal) peripheral curve** for M at T if $c = \partial S$ for some properly-embedded surface $S \subset C$ (resp. $S \subset Cl(S^3 \setminus C)$).

In order to translate the computation of composite knot symmetries from topology to combinatorics we will define a tree associated to a composite knot. The well-definedness of this construction will depend on the following proposition which will be stated without proof. The interested reader is directed to proposition 2.4 of Budney [Bud06] for more information.

Proposition 49 (cf. Budney [Bud06])**.** *Let $M \subset S^3$ be a 3-manifold whose boundary is a disjoint union of tori. Up to isotopy, there exists a unique orientation preserving embedding $f : M \to S^3$ such that the following are true:*

1. *$f(M)$ is the complement of a tubular neightborhood of a link in S^3.*

2. *f maps external peripheral curves of ∂M to external peripheral curves of $\partial(f(M))$.*

f is called the untwisted reimbedding of M.

Definition 50. Let L be a link in S^3, if $M \subset C_L$ is a manifold with incompressible torus boundary let $f : M \to S^3$ be its untwisted re-embedding. Then $f(M)$ is the complement of a link L' in S^3. Since f is unique up to isotopy, so is L'. Any such link will be called a **companion** to L.

Given a knot K we can decompose C_K by embedding solid tori $\cup T_i$ as shown in Figure 5.1. Note that these tori are in bijection with the prime factors of K.

Definition 51. We denote by H^p the $(p+1)$-component **key chain link** (shown below) such that all pair-wise linking numbers are $+1$. We also use the component labelings shown. We denote the ith component of H^p by H^p_i.

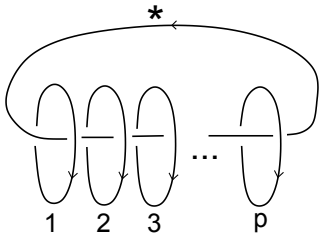

Lemma 52. *The companion link of K associated to $C_K \setminus \cup T_i$ is the key chain link H^k and the companion of the other 3-cell with boundary $\cup T_i$ is the split link of the prime factors of K as shown in Figure 5.1.*

Proof. This is a restatement of theorem 4.18 and corollary 4.19 in Budney [Bud06]. □

Definition 53. A **prime decomposition tree** is a depth one rooted tree $\mathbb{PG}(K)$ with root labeled by the link H^p whose children are ordered vertices labeled by oriented prime knots

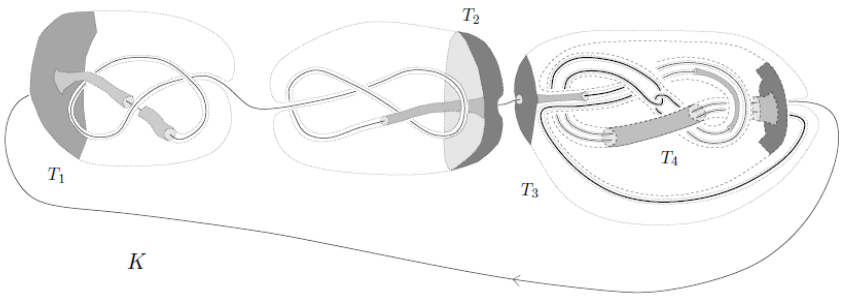

Figure 5.1: A figure from Budney [Bud06] showing the JSJ-decomposition of a composite knot. The tori T_1, T_2, and T_3 are the tori from Lemma 52. Notice that there are possibly additional tori in the JSJ-decomposition, but these are not adjacent to the knot complement C_k. The torus T_4 here is an example.

(see Figure 5.2). We denote the knot corresponding to vertex v by $\mathbb{PG}(v)$. We say that two prime decomposition trees $\mathbb{PG}$ and $\mathbb{PG}'$ are equivalent, denoted $\mathbb{PG} \sim \mathbb{PG}'$, if there exists an isomorphism of rooted trees $g : \mathbb{PG} \to \mathbb{PG}'$ such that $\mathbb{PG}(v) \sim \mathbb{PG}'(g(v))$

Proposition 54. *Two knots K_1 and K_2 are isotopic if and only if $\mathbb{PG}(K_1) \sim \mathbb{PG}(K_2)$.*

Proof. First, suppose that $K_1 \sim K_2$. Then there is an isotopy h from K_1 to K_2. We know that $\cup T_i$ are in the JSJ-decomposition of C_{K_1} by corollary 4.19 in Budney [Bud06]. Since the JSJ-decomposition is unique up to isotopy we have that if T is in the JSJ-decomposition of C_{K_1}, then $h(T)$ is in the JSJ-decomposition of K_2. If M is a 3-cell in C_{K_1} split along $\cup T_i$, then $h(M)$ is a 3-cell in C_{K_2} split along $\cup h(T_i)$ which is isotopic to M. Thus by Proposition 49, the companion link of M is isotopic to the companion link of $h(M)$. We can therefore build a isomorphism of rooted trees with corresponding isotopies of links.

The converse is immediate because JSJ-decompositions and companion links are unique up to isotopy. □

A knot can be recovered from a prime decomposition tree via the splicing operation.

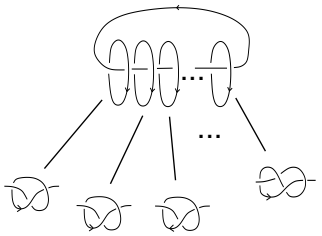

Figure 5.2: An example of a prime decompostion tree.

Definition 55. A **long knot** is an embedding $f : \mathbb{R} \times D^2 \to \mathbb{R} \times D^2$ such that:

1. f is the identity outside of $[-1, 1] \times D^2$.

2. $lk(f_{|\mathbb{R}\times\{(0,0)\}}, f_{|\mathbb{R}\times\{(1,0)\}}) = 0$

Long knots are in one-to-one correspondence with knots in S^3. A proof can be found in Budney [Bud07].

We will now define a special case of the splicing operation which corresponds to connected sums.

Definition 56. Let $I = [-\infty, \infty]$ and H^p be as above. Let $C_u = \cap_{i=1}^p C_{H_i^p}$ and $h = (h_1, \ldots, h_p)$ be a collection of disjoint orientation preserving embeddings $h_i : I \times D^2 \to C_{H_i^p}$ such that $img(h_i) \cap \partial C_u = img(h_{i|I\times\partial D^2})$ with $h_i(\{0\} \times S^1)$ an oriented longitude for L_i.

Given $K = (K_1, \ldots, K_p)$ a p-tuple of non-trivial knots in S^3, let $f = (f_1, \ldots, f_p)$ be the corresponding longs knots. We define the re-embedding function associated to L, h, and K to be

$$R_h[H^p, K] := \begin{cases} (h_i \circ f_i \circ h_i^{-1}), & \text{if } x \in img(h_i) \\ x, & \text{if } x \in C_u \setminus \sqcup_{i=1}^p img(h_i) \end{cases}$$

The **splice** of K along H^p is defined to be

$$K \rtimes H^p := R_h[H^p, K](*)$$

This definition seems to depend on the choice of h, but this is not the case. See Budney for the proof of the independence on h.

Proposition 57 (cf. Budney [Bud06] Corollary 4.19)**.** *$K \rtimes H^p$ is isotopic to $K_1 \# \ldots \# K_p$.*

Thus, the splicing operation can be used to recover a knot from a prime decomposition tree. If $\mathbb{PG}$ is a prime decomposition tree, then we denote the knot obtained by splicing $S(\mathbb{PG})$.

Theorem 58. *If $\mathbb{PG}$ and $\mathbb{PG}'$ are prime decomposition trees, then $S(\mathbb{PG}) \sim S(\mathbb{PG}')$ if and only if $\mathbb{PG} \sim \mathbb{PG}'$.*

Proof. Suppose that $S(\mathbb{PG}) \sim S(\mathbb{PG}')$, then by Proposition 54 we have that $\mathbb{PG}(S(\mathbb{PG})) \sim \mathbb{PG}'(S(\mathbb{PG}))$. But, by the uniqueness of the prime factorization of knots there is a permutation of the leaves of $\mathbb{PG}(S(\mathbb{PG}))$ so that we obtain $\mathbb{PG}$ and similarly for $\mathbb{PG}'$. Thus, $\mathbb{PG} \sim \mathbb{PG}'$.

On the other hand if $\mathbb{PG} \sim \mathbb{PG}'$, then by associativity of the connected sum of knots and Proposition 57 we have that $S(\mathbb{PG}) \sim S(\mathbb{PG}')$. □

We end this chapter with the observation that Γ has an action on prime decomposition trees induced by the action of Γ on the pair (S^3, K).

Definition 59. Given a prime decomposition tree $\mathbb{PG}(K)$ and $\gamma \in \Gamma$ we define $\gamma(\mathbb{PG}(K))$ to be the tree whose ordered leaves are the knots $\gamma(K_i)$ where the K_i are the labels of $\mathbb{PG}(K)$.

Chapter 6

Prime Diagram Trees

Lemma 45 ensures the existence of a preferred list of PD-code which we will refer to from now on by **the prime knot table**. We will use the prime knot table to define a combinatorial object analogous to the prime decomposition tree that will play a key role in the computation of symmetries and the tabulation of composite knots.

Definition 60. A **prime diagram tree** is a depth 1 rooted tree whose vertices are ordered and labeled by PD-codes from the prime knot table. We denote the PD-code at vertex v by PD(v) and the corresponding knot $k(v)$. The vertices respect a chosen ordering on base types so that if $i \leq j$, then $k(v_i) \leq k(v_j)$. We say that two prime diagram trees T_1 and T_2 are equivalent (denoted $T_1 \sim T_2$) if there is an isomorphism of trees $\phi : T_1 \to T_2$ such that $k(\phi(v)) \sim k(v)$ for every vertex $v \in T_1$.

Definition 61. Given a prime diagram tree T we construct a single PD-code by taking the connected sum of the PD-codes as describe in Definition 41 of the leaves in the order given by the tree. The PD-code constructed in this manner will be denoted PD(T) and the knot corresponding to this PD-code $k(T)$.

Proposition 62. *If T_1 and T_2 are prime diagram trees, then $k(T_1) \sim k(T_2)$ if and only if $T_1 \sim T_2$.*

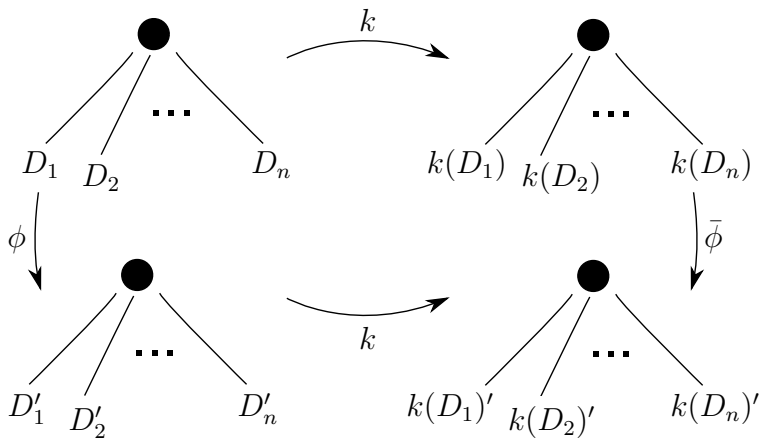

Figure 6.1: Trees of diagrams mapping to trees of knots.

Proof. Suppose that $k(T_1) \sim k(T_2)$. Then by the uniqueness of prime factorization there is a reordering of the leaves of related any two prime diagram trees associated to the knots. Thus, $T_1 \sim T_2$.

Suppose now that $T_1 \sim T_2$. Then by the associativity of the connected sum we have that $k(T_1) \sim k(T_2)$.

□

We can therefore consider prime diagram trees instead of prime decomposition trees.

Definition 63. Let $\mathbb{T}$ be the collection of prime diagram trees whose vertices are labeled by diagrams from the prime knot table.

We now introduce our conventions for indexing the prime factors of a knot and define the action of Γ on a prime diagram tree.

Definition 64. A **base prime factor list** $P = \{(D_i, n_i)\}_{i=1}^{l}$ is a set of PD-codes from the prime knot table along with multiplicities. We say that P is the base prime factor list for a knot k if the base types of the prime factors of k appear in P with the correct multiplicities.

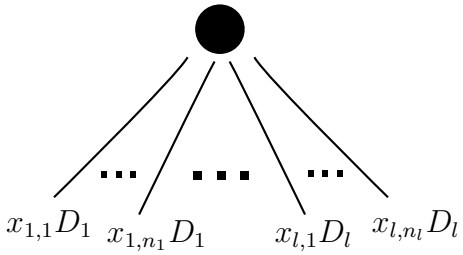

Figure 6.2: The prime diagram tree associated to $P = \{(D_i, n_i)\}_{i=1}^{l}$ and $x = ((x_{1,1}, \ldots, x_{1,n_1}), \ldots, (x_{l,1}, \ldots, x_{l,n_l}))$.

Definition 65. The collection of all prime diagram trees whose leaves are labeled by knots whose base types are exactly the base prime factor list P will be denoted $\mathbb{T}(P)$.

Definition 66. Let $X(P)$ be the set $\{\times_{i=1}^{l}\Gamma^{n_i}\}$.

Lemma 67. *$X(P)$ is in bijection with $\mathbb{T}(P)$.*

Proof. The correspondence is given by associating $x = ((x_{1,1}, \ldots, x_{1,n_1}), \ldots, (x_{l,1}, \ldots, x_{l,n_l}))$ with the prime diagram tree whose children are $x_{1,1}D_1, \ldots, x_{1,n_1}D_1, \ldots, x_{l,1}D_l, \ldots, x_{l,n_l}D_l$ (cf. Figure 6.2). We will denote this tree by $\mathbb{T}(x)$.

□

Definition 68. We define the group $\Gamma(P)$ by

$$\Gamma(P) := \oplus_{i=1}^{l} [(\oplus_{n_i}\Gamma) \rtimes S_{n_i}]$$

and the group $\Sigma(P)$ by

$$\Sigma(P) := \oplus_{i=1}^{l} [(\oplus_{n_i}\Sigma(k_i)) \rtimes S_{n_i}]$$

Definition 69. There is a natural action of $\Gamma(P)$ on $X(P)$ given by the following.

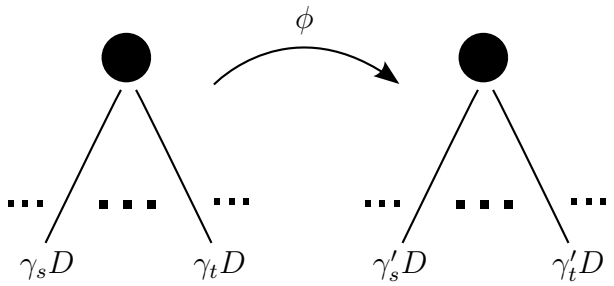

Figure 6.3: A map of prime diagram trees.

$$((\gamma_{1,1},\ldots,\gamma_{1,n_1},p_1),\ldots,(\gamma_{l,1},\ldots,\gamma_{l,n_l},p_l)) * ((x_{1,1},\ldots,x_{1,n_1}),\ldots,(x_{l,1},\ldots,x_{l,n_l}))$$

$$= ((\gamma_{1,1}x_{1,p_1(1)},\ldots,\gamma_{1,n_1}x_{1,p_1(n_1)}),\ldots,(\gamma_{l,1}x_{1,p_l(1)},\ldots,\gamma_{l,n_l}x_{l,p_l(n_l)}))$$

By factoring through the bijection of Proposition 35 we have an induced action of $\Gamma(P)$ on $\mathbb{T}(P)$.

6.1 The Enhanced Prime Decomposition Theorem

Proposition 70. *$\mathbb{T}(x) \sim \mathbb{T}(x')$ if and only if there exists $\sigma \in \Sigma(P)$ such that $\sigma(x) = x'$.*

Proof. First suppose that $\mathbb{T}(x) \sim \mathbb{T}(x')$. So, there is an isomorphism of trees ϕ with corresponding isotopies between $k(v)$ and $k(\phi(v))$. Let p be the permutation element corresponding to the action of ϕ on the leaves of $\mathbb{T}(x)$. Since two vertices cannot be permuted if they have different base type we see that $p = p_1 \cdots p_l \in \oplus_i S_{n_i}$. Within the leaves corresponding to a particular base type if $p(s) = t$, then $\gamma_s k \sim \gamma'_t k$ and $\gamma'_s k \sim \gamma_t k$.

Note that this implies that γ_s and γ'_t are in the same right $\Sigma(k)$ coset of Γ as the action of $\Sigma(k)$ is a left action. Consider the element $(\ldots,\gamma'_s\gamma_t^{-1},\ldots,\gamma'_t\gamma_s^{-1},\ldots,p_i)$ and note that this element corresponds to the transposition of vertices s and t induced by ϕ. We now

claim that $\gamma'_s\gamma_t^{-1}$ and $\gamma'_t\gamma_s^{-1}$ are in $\Sigma(k)$. Since γ'_s and γ_t are in the same right $\Sigma(k)$ coset we have that $\gamma'_s = \sigma'\gamma$ and $\gamma_t = \sigma\gamma$. Thus, $\gamma'_s\gamma_t^{-1} = \sigma'\gamma\gamma^{-1}\sigma^{-1} = \sigma'\sigma^{-1} \in \Sigma(k)$. Similarly, $\gamma'_t\gamma_s^{-1} \in \Sigma(k)$ and we can therefore repeat this process for each pair of vertices and construct $g \in \Sigma(P)$ that realizes the action of ϕ.

Now conversely suppose that there is some $\sigma \in \Sigma(P)$ such that $\sigma(x) = x'$. If $\sigma = ((\gamma_{1,1}, \ldots, \gamma_{1,n_1}, p_1), \ldots, (\gamma_{l,1}, \ldots, \gamma_{l,n_l}, p_l))$ then permuting the leaves of $T(x)$ by the permutations p_i only permutes leaves of the same base type and since each $\gamma_{i,j} \in \Sigma(k_i)$ we have that permuted vertices are equivalent PD-codes. Thus, σ induces an isomorphism of decomposition trees and so $\mathbb{T}(x) \sim \mathbb{T}(x')$. □

Lemma 71. *The map k descends to a surjective map from the $\Sigma(P)$ orbits of $\mathbb{T}(P)$ to knot types whose base prime factor list is P.*

Proof. We first show that k descends to a map on the $\Sigma(P)$ orbits of $\mathbb{T}(P)$. Suppose T and T' are in the same orbit, so there exists a $\sigma \in \Sigma(P)$ such that $\sigma T = T'$. Thus, by Proposition 70 we have that $T \sim T'$. So, by Proposition 62 $k(T) \sim k(T')$ and we see that k descends to a map on $\Sigma(P)$ orbits.

Since every knot has a prime factorization and the action of Γ on each base type is transitive by definition we see that k is surjective. □

Theorem 72. *The orbits of the $\Sigma(P)$ action on $X(P)$ are in bijection with the isotopy classes of knots whose base prime factor list is P.*

Proof. First note that the $\Sigma(P)$ orbits of $X(P)$ are the same as the $\Sigma(P)$ orbits of $\mathbb{T}(P)$ by construction. Proposition 70 shows that the $\Sigma(P)$ orbits on $\mathbb{T}(P)$ is the partition associated to the equivalence on prime decomposition trees. Thus, the result follows from Proposition 62.

□

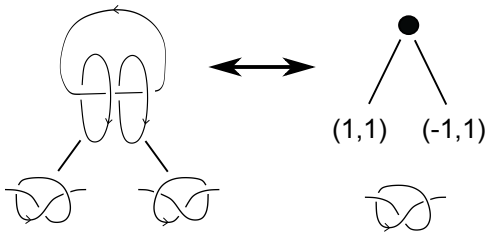

Figure 6.4: A prime decomposition tree and its associated tree labeled by Γ.

Definition 73. We can now define Orbit(K) to be the orbit in $X(P)$ which corresponds to the knot K under this bijection.

Example 74. Consider the base prime factor list $P = \{3_1, 2\}$ where 3_1 denotes the PD-code of the standard diagram of the trefoil of Figure 3.2. This corresponds to taking the connected sum of 2 trefoils. The trefoil is an invertible, chiral knot so $\Sigma(3_1) = \{(1,1),(1,-1)\}$. Therefore,

$$\Sigma(\{3_1, 2\}) = (\Sigma(3_1) \oplus \Sigma(3_1)) \rtimes S_2 = (\{(1,1),(1,-1)\} \oplus \{(1,1),(1,-1)\}) \rtimes S_2,$$

and

$$X(\{3_1, 2\}) = \Gamma \times \Gamma.$$

The orbits of the action of $\Sigma(\{3_1, 2\})$ on $X(\{3_1, 2\})$ are shown in Figure 6.5. There are 3 isotopy classes of composite knots that can be constructed from 2 trefoils. They are the right and left handed granny knots and the square knot.

Composite	Orbit	
Granny Knot	$((1,1),(1,1))$	$((1,-1),(1,1))$
	$((1,1),(1,-1))$	$((1,-1),(1,-1))$
Square Knot	$((1,1),(-1,1))$	$((1,-1),(-1,1))$
	$((1,1),(-1,-1))$	$((1,-1),(-1,-1))$
	$((-1,1),(1,1))$	$((-1,-1),(1,1))$
	$((-1,1),(1,-1))$	$((-1,-1),(1,-1))$
Granny Knot	$((-1,1),(-1,1))$	$((-1,-1),(-1,1))$
	$((-1,1),(-1,-1))$	$((-1,-1),(-1,-1))$

Figure 6.5: The orbits of the action of Γ corresponding to the isotopy classes of $3_1\#3_1$ of Example 74.

Chapter 7

Symmetries of Composite Knots

We now turn to the task of computing the intrinsic symmetries of a composite knot from those of its prime factors. Table 7.1 gives the occurrences of each symmetry type among the 544 composite knots through 12 crossings. The results in this section justify the computation which is explained in Chapter 8.

Definition 75. We define Δ to be the following subgroup of $\Gamma(P)$.

$$\Delta := \{((\gamma, \ldots, \gamma, p_1), \ldots, (\gamma, \ldots, \gamma, p_l)) | \gamma \in \Gamma, p_i \in S_{n_i}\}$$

The following lemma is immediate.

Lemma 76. *The map* $\pi : \Delta \to \Gamma$ *given by*

$$((\gamma, \ldots, \gamma, p_1), \ldots, (\gamma, \ldots, \gamma, p_l)) \mapsto \gamma$$

is a surjection.

By restricting the action of $\Gamma(P)$ to the subgroup Δ and factoring through the map of Lemma 76 we have a well-defined action of Γ on prime diagram trees which corresponds with the action of Γ on knots.

The following theorem gives the symmetry group of a composite knot.

Theorem 77.

$$\Sigma(K) = \pi(\Delta \cap \mathrm{Stab}\,(\mathrm{Orbit}(K)))$$

Proof. First note that if $\sigma \in \Sigma(K)$ then the element $\bar{\sigma} := ((\sigma, \ldots, \sigma, id), \ldots, (\sigma, \ldots, \sigma, id)) \in \Delta$ must stabilize $\mathrm{Orbit}(K)$ by Theorem 72 as $K \sim \sigma(K)$. Since $\pi(\bar{\sigma}) = \sigma$ we have that $\Sigma(k) \subset \pi(\Delta \cap \mathrm{Stab}\,(\mathrm{Orbit}(K)))$.

Now suppose that $\gamma \in \pi(\Delta \cap \mathrm{Stab}\,(\mathrm{Orbit}(K)))$. We must show that $K \sim \gamma(K)$. First note that elements of the form $(((1,1), \ldots, (1,1), q_1), \ldots, ((1,1), \ldots, (1,1), q_k))$ always act trivially for any choice of the permutations q_i since the connected sum of knots is commutative. Thus we may assume that $((\gamma, \ldots, \gamma, id), \ldots, (\gamma, \ldots, \gamma, id)) \in \mathrm{Stab}\,(\mathrm{Orbit}(K))$. But, $\pi(((\gamma, \ldots, \gamma, id), \ldots, (\gamma, \ldots, \gamma, id))) = \gamma$. Thus, $\gamma \in \Sigma(K)$. □

It is interesting to compare Theorem 77 with Theorem 2 of Whitten [WCW69]. While it is possible to compute the group $\Sigma(K)$ from Whitten's theorem, it is much easier to construct an algorithm that implements the group action of $\Gamma(K)$ on $X(P)$ than to implement a verification of the conditions of Whitten. Moreover, the statement of the Theorem 77 is greatly simplified because the combinatorics of Whitten's indices are encoded in the action of $\Gamma(P)$ on $X(P)$. Another advantage is that Theorem 77 describes the entire group $\Sigma(K)$ rather than just giving necessary and sufficient conditions for an element to be a symmetry.

There are several immediate corollaries to Theorem 77 which predict symmetries of a composite knot from the symmetries of the prime factors. We first discuss a generalization of the square knot from Example 74.

Corollary 78. *Suppose K is a composite knot with prime factors $\{K_1, \ldots, K_n\}$ such $\Sigma(K_i) = \Gamma$ for all i, then $\Sigma(K) = \Gamma$.*

Definition 79. K is a **generalized square knot** if the prime factors for K are

$$\{K_1, \gamma_1 K_1, \ldots, K_1, \gamma_1 K_1\}$$

where $\Sigma(K_1) =< \gamma_2 >$ and $\Gamma =< \gamma_1, \gamma_2 >$.

Corollary 80. *Suppose K is a generalized square knot, then $\Sigma(K) = \Gamma$.*

Corollary 80 could be thought of as an application of the following which gives sufficient conditions for a 2 factor summand to admit a symmetry.

Corollary 81. *Suppose $K = K_1 \# \gamma K_1$, then $\gamma \in \Sigma(K)$.*

We can produce a knot with full symmetry by taking the connected sum of each flavor of base type.

Corollary 82. *Suppose $K = K_1 \# \gamma_1 K_1 \# \gamma_2 K_1 \# \gamma_3 K_1$ with $\gamma_1, \gamma_2, \gamma_3$ all distinct, then $\Sigma(K) = \Gamma$.*

If K has no symmetry, then iterated connected sums of K will also have no symmetry.

Corollary 83. *Suppose K has no symmetry. Then $K \# \cdots \# K$ has no symmetry.*

Symmetry Type	Number of Occurrences
No Symmetry	20
(+) Amphichiral Symmetry	2
Invertible Symmetry	506
(-) Amphichiral Symmetry	0
Full Symmetry	16

Figure 7.1: The number of each symmetry type among the 544 composite knots of up to 12 crossings.

Chapter 8

Composite Knot Tabulation

The action of $\Gamma(P)$ on $X(P)$ (cf. Definitions 68 and 66) can be implemented in `Mathematica` to generate the composite knot tables. Theorem 72 implies that the only information needed to compute the isotopy classes are which factors are of the same base type and what the symmetry group of each factor base type is. It is therefore natural to organize tables by this information. These tables are contained in Chapter 9. The implementation of the action of $\Gamma(P)$ on $X(P)$ will now be discussed.

8.1 Implementing the Action of $\Gamma(P)$ on $X(P)$

The implementation of the Action of $\Gamma(P)$ on $X(P)$ depends on the `KnotTheory` package written by Dror Bar-Natan [BN11] and the `whitten.m` package written by Jason Cantarella. The `KnotTheory` package implements many computational tools including methods to draw link diagrams from PD-codes as well as many methods for computing links invariants. The `whitten.m` package implements the algebra of the group Γ_μ and its action on PD-codes.

The multiplication in Γ is simply component-wise multiplication and can be implemented by the following code.

```
WhitMult[x_, y_] := {x[[1]]*y[[1]], x[[2]]*y[[2]]};
```

To implement the action of $\Gamma(P)$ on $X(P)$ we first define the action on each direct summand. This is realized as the following.

```
ASigOnX[s_, x_] := Table[
   WhitMult[
    s[[i]],
    x[[
      s[[Length[s]]]
       [[i]]
      ]]
    ],
   {i, 1, Length[x]}];
```

The general action is then obtained by applying the previous method to each summand.

```
SigOnX[s_, x_] := Table[ASigOnX[s[[i]], x[[i]]], {i, 1, Length[x]}];
```

To compute all of the orbits we iterate over the previous function. We must take into account that duplicate elements will be found.

```
ComputeOrbits[P_] := Module[{x, sig, Orbs},
   x = XGen[P];
   sig = SigGen[P];
   Orbs =
    DeleteDuplicates[
     Sort[Table[
       DeleteDuplicates[
```

```
Sort[Table[
  SigOnX[sig[[i]], x[[j]]], {i, 1, Length[sig]}]], {j, 1,
Length[x]}], Greater]]];
```

We will now revisit the example of the connected sum of two trefoils.

Example 84. Consider the composite knots obtained by taking the connected sum of two trefoils. The trefoil enjoys invertible symmetry, so its symmetry group is $\{(1,1),(1,-1)\}$. We represent the this connected sum with the following base prime factor list.

```
{2, {{1, 1}, {1, -1}}}
```

We can compute the orbits with the following call.

```
ComputeOrbits[{{2, {2, {{1, 1}, {1, -1}}}}}];
```

The output of this call is a list of orbits.

```
{{{{{1, -1}, {1, -1}}}, {{{1, -1}, {1, 1}}}, {{{1,1}, {1, -1}}},
 {{{1, 1}, {1,1}}}}, {{{{-1, -1}, {1, -1}}}, {{{-1, -1}, {1, 1}}},
 {{{-1,1}, {1, -1}}}, {{{-1, 1}, {1,1}}}, {{{1, -1}, {-1, -1}}},
 {{{1, -1}, {-1, 1}}}, {{{1,1}, {-1, -1}}}, {{{1, 1}, {-1,1}}}},
{{{{-1, -1}, {-1, -1}}}, {{{-1, -1}, {-1, 1}}}, {{{-1,1}, {-1, -1}}},
 {{{-1, 1}, {-1, 1}}}}}
```

This is a bit hard to read, so we can choose a representative from each orbit.

```
{{1, 1}, {1, 1}}
{{1, 1}, {-1, 1}}
{{-1, 1}, {-1, 1}}
```

The first and last represent the two granny knots and the middle represents the square knot. Note that this agrees with the result from Example 74.

Now that we can tabulate the composite knots we turn to implementing an algorithm for determining the symmetry group of a composite knot. Theorem 77 tells us the the symmetry group of a composite knot is the intersection of the group

$$\Delta := \{((\gamma, \ldots, \gamma, p_1), \ldots, (\gamma, \ldots, \gamma, p_l))|\gamma \in \Gamma, p_i \in S_{n_i}\}$$

with the stabilizer of the orbit corresponding to the composite knot. For a particular orbit we can compute which elements of Δ are in the stabilizer with the following method.

```
CompSymSingle[P_, Orb_] := Module[{Diag, flag, i, j, SymGroup},
   Diag = SigDiagGen[P];
   SymGroup = {};
   For[i = 1, i <= Length[Diag], i++,
    flag = 1;
    For[j = 1, j <= Length[Orb], j++,
     If[Count[Orb, SigOnX[Diag[[i]], Orb[[j]]]] == 1, flag = 1,
      flag = 0, flag = 0];
     If[flag == 0, Break, True];
     ];
    If[flag == 1, AppendTo[SymGroup, Diag[[i]]], flag = 0];
    ];
   DeleteDuplicates[
    Table[Proj[SymGroup[[i]]], {i, 1, Length[SymGroup]}]]
   ];
```

Iterating over a list of orbits allows us to compute the symmetry types for all knots with a given base prime factor list.

```
CompSym[P_, Orbs_] :=
          Table[CompSymSingle[P, Orbs[[i]]], {i, 1, Length[Orbs]}];
```

Example 85. We again look at the two trefoil example. The symmetry groups are computed to be the following.

```
{{{1, 1}, {1, -1}},
 {{1, 1}, {-1, 1}, {1, -1}, {-1, -1}},
 {{1, 1}, {1, -1}}}
```

So, we see that the two granny knots have reversible symmetry while the square knot has full symmetry.

Chapter 9

Composite Knot Tables

In this chapter we present the table of composite links through 12 crossings along with their symmetry groups. The data was computed using the methods described in Chapter 8 and the tables were generated using a `perl` script written by Jason Cantarella. The tables presented here match and serve as a verification for the table of composite knots found in Cantarella, Rawdon, and LaPointe [Can12].

Table 9.1: Composite Knot Types, Part 1 of 6

Knot	Symmetry
$3_1\#3_1$	Invertible
$3_1\#3_1^m$	Full
$3_1^m\#3_1^m$	Invertible
$3_1\#4_1$	Invertible
$3_1^m\#4_1$	Invertible
$3_1\#5_1$	Invertible
$3_1\#5_1^m$	Invertible
$3_1^m\#5_1$	Invertible
$3_1^m\#5_1^m$	Invertible
$3_1\#5_2$	Invertible
$3_1\#5_2^m$	Invertible
$3_1^m\#5_2$	Invertible
$3_1^m\#5_2^m$	Invertible
$4_1\#4_1$	Full
$3_1\#6_1$	Invertible
$3_1\#6_1^m$	Invertible
$3_1^m\#6_1$	Invertible
$3_1^m\#6_1^m$	Invertible
$3_1\#6_2$	Invertible
$3_1\#6_2^m$	Invertible
$3_1^m\#6_2$	Invertible
$3_1^m\#6_2^m$	Invertible
$3_1\#6_3$	Invertible
$3_1^m\#6_3$	Invertible
$4_1\#5_1$	Invertible
$4_1\#5_1^m$	Invertible
$4_1\#5_2$	Invertible
$4_1\#5_2^m$	Invertible
$3_1\#3_1\#3_1$	Invertible
$3_1\#3_1\#3_1^m$	Invertible
$3_1\#3_1^m\#3_1^m$	Invertible
$3_1^m\#3_1^m\#3_1^m$	Invertible

Knot	Symmetry
$3_1\#7_1$	Invertible
$3_1\#7_1^m$	Invertible
$3_1^m\#7_1$	Invertible
$3_1^m\#7_1^m$	Invertible
$3_1\#7_2$	Invertible
$3_1\#7_2^m$	Invertible
$3_1^m\#7_2$	Invertible
$3_1^m\#7_2^m$	Invertible
$3_1\#7_3$	Invertible
$3_1\#7_3^m$	Invertible
$3_1^m\#7_3$	Invertible
$3_1^m\#7_3^m$	Invertible
$3_1\#7_4$	Invertible
$3_1\#7_4^m$	Invertible
$3_1^m\#7_4$	Invertible
$3_1^m\#7_4^m$	Invertible
$3_1\#7_5$	Invertible
$3_1\#7_5^m$	Invertible
$3_1^m\#7_5$	Invertible
$3_1^m\#7_5^m$	Invertible
$3_1\#7_6$	Invertible
$3_1\#7_6^m$	Invertible
$3_1^m\#7_6$	Invertible
$3_1^m\#7_6^m$	Invertible
$3_1\#7_7$	Invertible
$3_1\#7_7^m$	Invertible
$3_1^m\#7_7$	Invertible
$3_1^m\#7_7^m$	Invertible
$4_1\#6_1$	Invertible
$4_1\#6_1^m$	Invertible
$4_1\#6_2$	Invertible
$4_1\#6_2^m$	Invertible
$4_1\#6_3$	Full
$5_1\#5_1$	Invertible

Knot	Symmetry
$5_1\#5_1^m$	Full
$5_1^m\#5_1^m$	Invertible
$5_1\#5_2$	Invertible
$5_1\#5_2^m$	Invertible
$5_1^m\#5_2$	Invertible
$5_1^m\#5_2^m$	Invertible
$5_2\#5_2$	Invertible
$5_2\#5_2^m$	Full
$5_2^m\#5_2^m$	Invertible
$3_1\#3_1\#4_1$	Invertible
$3_1\#3_1^m\#4_1$	Full
$3_1^m\#3_1^m\#4_1$	Invertible
$3_1\#8_1$	Invertible
$3_1\#8_1^m$	Invertible
$3_1^m\#8_1$	Invertible
$3_1^m\#8_1^m$	Invertible
$3_1\#8_2$	Invertible
$3_1\#8_2^m$	Invertible
$3_1^m\#8_2$	Invertible
$3_1^m\#8_2^m$	Invertible
$3_1\#8_3$	Invertible
$3_1^m\#8_3$	Invertible
$3_1\#8_4$	Invertible
$3_1\#8_4^m$	Invertible
$3_1^m\#8_4$	Invertible
$3_1^m\#8_4^m$	Invertible
$3_1\#8_5$	Invertible
$3_1\#8_5^m$	Invertible
$3_1^m\#8_5$	Invertible
$3_1^m\#8_5^m$	Invertible
$3_1\#8_6$	Invertible
$3_1\#8_6^m$	Invertible
$3_1^m\#8_6$	Invertible
$3_1^m\#8_6^m$	Invertible

Table 9.2: Composite Knot Types, Part 2 of 6

Knot	Symmetry
$3_1\#8_7$	Invertible
$3_1\#8_7^m$	Invertible
$3_1^m\#8_7$	Invertible
$3_1^m\#8_7^m$	Invertible
$3_1\#8_8$	Invertible
$3_1\#8_8^m$	Invertible
$3_1^m\#8_8$	Invertible
$3_1^m\#8_8^m$	Invertible
$3_1\#8_9$	Invertible
$3_1^m\#8_9$	Invertible
$3_1\#8_{10}$	Invertible
$3_1\#8_{10}^m$	Invertible
$3_1^m\#8_{10}$	Invertible
$3_1^m\#8_{10}^m$	Invertible
$3_1\#8_{11}$	Invertible
$3_1\#8_{11}^m$	Invertible
$3_1^m\#8_{11}$	Invertible
$3_1^m\#8_{11}^m$	Invertible
$3_1\#8_{12}$	Invertible
$3_1^m\#8_{12}$	Invertible
$3_1\#8_{13}$	Invertible
$3_1\#8_{13}^m$	Invertible
$3_1^m\#8_{13}$	Invertible
$3_1^m\#8_{13}^m$	Invertible
$3_1\#8_{14}$	Invertible
$3_1\#8_{14}^m$	Invertible
$3_1^m\#8_{14}$	Invertible
$3_1^m\#8_{14}^m$	Invertible
$3_1\#8_{15}$	Invertible
$3_1\#8_{15}^m$	Invertible
$3_1^m\#8_{15}$	Invertible
$3_1^m\#8_{15}^m$	Invertible
$3_1\#8_{16}$	Invertible
$3_1\#8_{16}^m$	Invertible

Knot	Symmetry
$3_1^m\#8_{16}$	Invertible
$3_1^m\#8_{16}^m$	Invertible
$3_1\#8_{17}$	None
$3_1\#8_{17}^r$	None
$3_1^m\#8_{17}$	None
$3_1^m\#8_{17}^r$	None
$3_1\#8_{18}$	Invertible
$3_1^m\#8_{18}$	Invertible
$3_1\#8_{19}$	Invertible
$3_1\#8_{19}^m$	Invertible
$3_1^m\#8_{19}$	Invertible
$3_1^m\#8_{19}^m$	Invertible
$3_1\#8_{20}$	Invertible
$3_1\#8_{20}^m$	Invertible
$3_1^m\#8_{20}$	Invertible
$3_1^m\#8_{20}^m$	Invertible
$3_1\#8_{21}$	Invertible
$3_1\#8_{21}^m$	Invertible
$3_1^m\#8_{21}$	Invertible
$3_1^m\#8_{21}^m$	Invertible
$4_1\#7_1$	Invertible
$4_1\#7_1^m$	Invertible
$4_1\#7_2$	Invertible
$4_1\#7_2^m$	Invertible
$4_1\#7_3$	Invertible
$4_1\#7_3^m$	Invertible
$4_1\#7_4$	Invertible
$4_1\#7_4^m$	Invertible
$4_1\#7_5$	Invertible
$4_1\#7_5^m$	Invertible
$4_1\#7_6$	Invertible
$4_1\#7_6^m$	Invertible
$4_1\#7_7$	Invertible

Knot	Symmetry
$4_1\#7_7^m$	Invertible
$5_1\#6_1$	Invertible
$5_1\#6_1^m$	Invertible
$5_1^m\#6_1$	Invertible
$5_1^m\#6_1^m$	Invertible
$5_1\#6_2$	Invertible
$5_1\#6_2^m$	Invertible
$5_1^m\#6_2$	Invertible
$5_1^m\#6_2^m$	Invertible
$5_1\#6_3$	Invertible
$5_1^m\#6_3$	Invertible
$5_2\#6_1$	Invertible
$5_2\#6_1^m$	Invertible
$5_2^m\#6_1$	Invertible
$5_2^m\#6_1^m$	Invertible
$5_2\#6_2$	Invertible
$5_2\#6_2^m$	Invertible
$5_2^m\#6_2$	Invertible
$5_2^m\#6_2^m$	Invertible
$5_2\#6_3$	Invertible
$5_2^m\#6_3$	Invertible
$3_1\#3_1\#5_1$	Invertible
$3_1\#3_1\#5_1^m$	Invertible
$3_1\#3_1^m\#5_1$	Invertible
$3_1\#3_1^m\#5_1^m$	Invertible
$3_1^m\#3_1^m\#5_1$	Invertible
$3_1^m\#3_1^m\#5_1^m$	Invertible
$3_1\#3_1\#5_2$	Invertible
$3_1\#3_1\#5_2^m$	Invertible
$3_1\#3_1^m\#5_2$	Invertible
$3_1\#3_1^m\#5_2^m$	Invertible
$3_1^m\#3_1^m\#5_2$	Invertible
$3_1^m\#3_1^m\#5_2^m$	Invertible
$3_1\#4_1\#4_1$	Invertible

Table 9.3: Composite Knot Types, Part 3 of 6

Knot	Symmetry
$3_1^m \# 4_1 \# 4_1$	Invertible
$3_1 \# 9_1$	Invertible
$3_1 \# 9_1^m$	Invertible
$3_1^m \# 9_1$	Invertible
$3_1^m \# 9_1^m$	Invertible
$3_1 \# 9_2$	Invertible
$3_1 \# 9_2^m$	Invertible
$3_1^m \# 9_2$	Invertible
$3_1^m \# 9_2^m$	Invertible
$3_1 \# 9_3$	Invertible
$3_1 \# 9_3^m$	Invertible
$3_1^m \# 9_3$	Invertible
$3_1^m \# 9_3^m$	Invertible
$3_1 \# 9_4$	Invertible
$3_1 \# 9_4^m$	Invertible
$3_1^m \# 9_4$	Invertible
$3_1^m \# 9_4^m$	Invertible
$3_1 \# 9_5$	Invertible
$3_1 \# 9_5^m$	Invertible
$3_1^m \# 9_5$	Invertible
$3_1^m \# 9_5^m$	Invertible
$3_1 \# 9_6$	Invertible
$3_1 \# 9_6^m$	Invertible
$3_1^m \# 9_6$	Invertible
$3_1^m \# 9_6^m$	Invertible
$3_1 \# 9_7$	Invertible
$3_1 \# 9_7^m$	Invertible
$3_1^m \# 9_7$	Invertible
$3_1^m \# 9_7^m$	Invertible
$3_1 \# 9_8$	Invertible
$3_1 \# 9_8^m$	Invertible
$3_1^m \# 9_8$	Invertible
$3_1^m \# 9_8^m$	Invertible
$3_1 \# 9_9$	Invertible
$3_1 \# 9_9^m$	Invertible
$3_1^m \# 9_9$	Invertible
$3_1^m \# 9_9^m$	Invertible
$3_1 \# 9_{10}$	Invertible
$3_1 \# 9_{10}^m$	Invertible
$3_1^m \# 9_{10}$	Invertible
$3_1^m \# 9_{10}^m$	Invertible
$3_1 \# 9_{11}$	Invertible
$3_1 \# 9_{11}^m$	Invertible
$3_1^m \# 9_{11}$	Invertible
$3_1^m \# 9_{11}^m$	Invertible
$3_1 \# 9_{12}$	Invertible
$3_1 \# 9_{12}^m$	Invertible
$3_1^m \# 9_{12}$	Invertible
$3_1^m \# 9_{12}^m$	Invertible
$3_1 \# 9_{13}$	Invertible
$3_1 \# 9_{13}^m$	Invertible
$3_1^m \# 9_{13}$	Invertible
$3_1^m \# 9_{13}^m$	Invertible
$3_1 \# 9_{14}$	Invertible
$3_1 \# 9_{14}^m$	Invertible
$3_1^m \# 9_{14}$	Invertible
$3_1^m \# 9_{14}^m$	Invertible
$3_1 \# 9_{15}$	Invertible
$3_1 \# 9_{15}^m$	Invertible
$3_1^m \# 9_{15}$	Invertible
$3_1^m \# 9_{15}^m$	Invertible
$3_1 \# 9_{16}$	Invertible
$3_1 \# 9_{16}^m$	Invertible
$3_1^m \# 9_{16}$	Invertible
$3_1^m \# 9_{16}^m$	Invertible
$3_1 \# 9_{17}$	Invertible
$3_1 \# 9_{17}^m$	Invertible
$3_1^m \# 9_{17}$	Invertible
$3_1^m \# 9_{17}^m$	Invertible
$3_1 \# 9_{18}$	Invertible
$3_1 \# 9_{18}^m$	Invertible
$3_1^m \# 9_{18}$	Invertible
$3_1^m \# 9_{18}^m$	Invertible
$3_1 \# 9_{19}$	Invertible
$3_1 \# 9_{19}^m$	Invertible
$3_1^m \# 9_{19}$	Invertible
$3_1^m \# 9_{19}^m$	Invertible
$3_1 \# 9_{20}$	Invertible
$3_1 \# 9_{20}^m$	Invertible
$3_1^m \# 9_{20}$	Invertible
$3_1^m \# 9_{20}^m$	Invertible
$3_1 \# 9_{21}$	Invertible
$3_1 \# 9_{21}^m$	Invertible
$3_1^m \# 9_{21}$	Invertible
$3_1^m \# 9_{21}^m$	Invertible
$3_1 \# 9_{22}$	Invertible
$3_1 \# 9_{22}^m$	Invertible
$3_1^m \# 9_{22}$	Invertible
$3_1^m \# 9_{22}^m$	Invertible
$3_1 \# 9_{23}$	Invertible
$3_1 \# 9_{23}^m$	Invertible
$3_1^m \# 9_{23}$	Invertible
$3_1^m \# 9_{23}^m$	Invertible
$3_1 \# 9_{24}$	Invertible
$3_1 \# 9_{24}^m$	Invertible
$3_1^m \# 9_{24}$	Invertible
$3_1^m \# 9_{24}^m$	Invertible
$3_1 \# 9_{25}$	Invertible
$3_1 \# 9_{25}^m$	Invertible
$3_1^m \# 9_{25}$	Invertible
$3_1^m \# 9_{25}^m$	Invertible
$3_1 \# 9_{26}$	Invertible
$3_1 \# 9_{26}^m$	Invertible
$3_1^m \# 9_{26}$	Invertible
$3_1^m \# 9_{26}^m$	Invertible

Table 9.4: Composite Knot Types, Part 4 of 6

Knot	Symmetry
$3_1^m \# 9_{26}^m$	Invertible
$3_1 \# 9_{27}$	Invertible
$3_1 \# 9_{27}^m$	Invertible
$3_1^m \# 9_{27}$	Invertible
$3_1^m \# 9_{27}^m$	Invertible
$3_1 \# 9_{28}$	Invertible
$3_1 \# 9_{28}^m$	Invertible
$3_1^m \# 9_{28}$	Invertible
$3_1^m \# 9_{28}^m$	Invertible
$3_1 \# 9_{29}$	Invertible
$3_1 \# 9_{29}^m$	Invertible
$3_1^m \# 9_{29}$	Invertible
$3_1^m \# 9_{29}^m$	Invertible
$3_1 \# 9_{30}$	Invertible
$3_1 \# 9_{30}^m$	Invertible
$3_1^m \# 9_{30}$	Invertible
$3_1^m \# 9_{30}^m$	Invertible
$3_1 \# 9_{31}$	Invertible
$3_1 \# 9_{31}^m$	Invertible
$3_1^m \# 9_{31}$	Invertible
$3_1^m \# 9_{31}^m$	Invertible
$3_1 \# 9_{32}$	None
$3_1 \# 9_{32}^r$	None
$3_1 \# 9_{32}^m$	None
$3_1 \# 9_{32}^{rm}$	None
$3_1^m \# 9_{32}$	None
$3_1^m \# 9_{32}^r$	None
$3_1^m \# 9_{32}^m$	None
$3_1^m \# 9_{32}^{rm}$	None
$3_1 \# 9_{33}$	None
$3_1 \# 9_{33}^r$	None
$3_1 \# 9_{33}^m$	None
$3_1 \# 9_{33}^{rm}$	None
$3_1^m \# 9_{33}$	None
$3_1^m \# 9_{33}^r$	None

Knot	Symmetry
$3_1^m \# 9_{33}^m$	None
$3_1^m \# 9_{33}^{rm}$	None
$3_1 \# 9_{34}$	Invertible
$3_1 \# 9_{34}^m$	Invertible
$3_1^m \# 9_{34}$	Invertible
$3_1^m \# 9_{34}^m$	Invertible
$3_1 \# 9_{35}$	Invertible
$3_1 \# 9_{35}^m$	Invertible
$3_1^m \# 9_{35}$	Invertible
$3_1^m \# 9_{35}^m$	Invertible
$3_1 \# 9_{36}$	Invertible
$3_1 \# 9_{36}^m$	Invertible
$3_1^m \# 9_{36}$	Invertible
$3_1^m \# 9_{36}^m$	Invertible
$3_1 \# 9_{37}$	Invertible
$3_1 \# 9_{37}^m$	Invertible
$3_1^m \# 9_{37}$	Invertible
$3_1^m \# 9_{37}^m$	Invertible
$3_1 \# 9_{38}$	Invertible
$3_1 \# 9_{38}^m$	Invertible
$3_1^m \# 9_{38}$	Invertible
$3_1^m \# 9_{38}^m$	Invertible
$3_1 \# 9_{39}$	Invertible
$3_1 \# 9_{39}^m$	Invertible
$3_1^m \# 9_{39}$	Invertible
$3_1^m \# 9_{39}^m$	Invertible
$3_1 \# 9_{40}$	Invertible
$3_1 \# 9_{40}^m$	Invertible
$3_1^m \# 9_{40}$	Invertible
$3_1^m \# 9_{40}^m$	Invertible
$3_1 \# 9_{41}$	Invertible
$3_1 \# 9_{41}^m$	Invertible
$3_1^m \# 9_{41}$	Invertible
$3_1^m \# 9_{41}^m$	Invertible

Knot	Symmetry
$3_1 \# 9_{42}$	Invertible
$3_1 \# 9_{42}^m$	Invertible
$3_1^m \# 9_{42}$	Invertible
$3_1^m \# 9_{42}^m$	Invertible
$3_1 \# 9_{43}$	Invertible
$3_1 \# 9_{43}^m$	Invertible
$3_1^m \# 9_{43}$	Invertible
$3_1^m \# 9_{43}^m$	Invertible
$3_1 \# 9_{44}$	Invertible
$3_1 \# 9_{44}^m$	Invertible
$3_1^m \# 9_{44}$	Invertible
$3_1^m \# 9_{44}^m$	Invertible
$3_1 \# 9_{45}$	Invertible
$3_1 \# 9_{45}^m$	Invertible
$3_1^m \# 9_{45}$	Invertible
$3_1^m \# 9_{45}^m$	Invertible
$3_1 \# 9_{46}$	Invertible
$3_1 \# 9_{46}^m$	Invertible
$3_1^m \# 9_{46}$	Invertible
$3_1^m \# 9_{46}^m$	Invertible
$3_1 \# 9_{47}$	Invertible
$3_1 \# 9_{47}^m$	Invertible
$3_1^m \# 9_{47}$	Invertible
$3_1^m \# 9_{47}^m$	Invertible
$3_1 \# 9_{48}$	Invertible
$3_1 \# 9_{48}^m$	Invertible
$3_1^m \# 9_{48}$	Invertible
$3_1^m \# 9_{48}^m$	Invertible
$3_1 \# 9_{49}$	Invertible
$3_1 \# 9_{49}^m$	Invertible
$3_1^m \# 9_{49}$	Invertible
$3_1^m \# 9_{49}^m$	Invertible
$4_1 \# 8_1$	Invertible
$4_1 \# 8_1^m$	Invertible

Table 9.5: Composite Knot Types, Part 5 of 6

Knot	Symmetry
$4_1\#8_2$	Invertible
$4_1\#8_2^m$	Invertible
$4_1\#8_3$	Full
$4_1\#8_4$	Invertible
$4_1\#8_4^m$	Invertible
$4_1\#8_5$	Invertible
$4_1\#8_5^m$	Invertible
$4_1\#8_6$	Invertible
$4_1\#8_6^m$	Invertible
$4_1\#8_7$	Invertible
$4_1\#8_7^m$	Invertible
$4_1\#8_8$	Invertible
$4_1\#8_8^m$	Invertible
$4_1\#8_9$	Full
$4_1\#8_{10}$	Invertible
$4_1\#8_{10}^m$	Invertible
$4_1\#8_{11}$	Invertible
$4_1\#8_{11}^m$	Invertible
$4_1\#8_{12}$	Full
$4_1\#8_{13}$	Invertible
$4_1\#8_{13}^m$	Invertible
$4_1\#8_{14}$	Invertible
$4_1\#8_{14}^m$	Invertible
$4_1\#8_{15}$	Invertible
$4_1\#8_{15}^m$	Invertible
$4_1\#8_{16}$	Invertible
$4_1\#8_{16}^m$	Invertible
$4_1\#8_{17}$	Mirror
$4_1\#8_{17}^r$	Mirror
$4_1\#8_{18}$	Full
$4_1\#8_{19}$	Invertible

Knot	Symmetry
$4_1\#8_{19}^m$	Invertible
$4_1\#8_{20}$	Invertible
$4_1\#8_{20}^m$	Invertible
$4_1\#8_{21}$	Invertible
$4_1\#8_{21}^m$	Invertible
$5_1\#7_1$	Invertible
$5_1\#7_1^m$	Invertible
$5_1^m\#7_1$	Invertible
$5_1^m\#7_1^m$	Invertible
$5_1\#7_2$	Invertible
$5_1\#7_2^m$	Invertible
$5_1^m\#7_2$	Invertible
$5_1^m\#7_2^m$	Invertible
$5_1\#7_3$	Invertible
$5_1\#7_3^m$	Invertible
$5_1^m\#7_3$	Invertible
$5_1^m\#7_3^m$	Invertible
$5_1\#7_4$	Invertible
$5_1\#7_4^m$	Invertible
$5_1^m\#7_4$	Invertible
$5_1^m\#7_4^m$	Invertible
$5_1\#7_5$	Invertible
$5_1\#7_5^m$	Invertible
$5_1^m\#7_5$	Invertible
$5_1^m\#7_5^m$	Invertible
$5_1\#7_6$	Invertible
$5_1\#7_6^m$	Invertible
$5_1^m\#7_6$	Invertible
$5_1^m\#7_6^m$	Invertible
$5_1\#7_7$	Invertible
$5_1\#7_7^m$	Invertible
$5_1^m\#7_7$	Invertible
$5_1^m\#7_7^m$	Invertible
$5_2\#7_1$	Invertible

Knot	Symmetry
$5_2\#7_1^m$	Invertible
$5_2^m\#7_1$	Invertible
$5_2^m\#7_1^m$	Invertible
$5_2\#7_2$	Invertible
$5_2\#7_2^m$	Invertible
$5_2^m\#7_2$	Invertible
$5_2^m\#7_2^m$	Invertible
$5_2\#7_3$	Invertible
$5_2\#7_3^m$	Invertible
$5_2^m\#7_3$	Invertible
$5_2^m\#7_3^m$	Invertible
$5_2\#7_4$	Invertible
$5_2\#7_4^m$	Invertible
$5_2^m\#7_4$	Invertible
$5_2^m\#7_4^m$	Invertible
$5_2\#7_5$	Invertible
$5_2\#7_5^m$	Invertible
$5_2^m\#7_5$	Invertible
$5_2^m\#7_5^m$	Invertible
$5_2\#7_6$	Invertible
$5_2\#7_6^m$	Invertible
$5_2^m\#7_6$	Invertible
$5_2^m\#7_6^m$	Invertible
$5_2\#7_7$	Invertible
$5_2\#7_7^m$	Invertible
$5_2^m\#7_7$	Invertible
$5_2^m\#7_7^m$	Invertible
$6_1\#6_1$	Invertible
$6_1\#6_1^m$	Full
$6_1^m\#6_1^m$	Invertible
$6_1\#6_2$	Invertible
$6_1\#6_2^m$	Invertible
$6_1^m\#6_2$	Invertible
$6_1^m\#6_2^m$	Invertible

Table 9.6: Composite Knot Types, Part 6 of 6

Knot	Symmetry
$6_1\#6_3$	Invertible
$6_1^m\#6_3$	Invertible
$6_2\#6_2$	Invertible
$6_2\#6_2^m$	Full
$6_2^m\#6_2^m$	Invertible
$6_2\#6_3$	Invertible
$6_2^m\#6_3$	Invertible
$6_3\#6_3$	Full
$3_1\#3_1\#6_1$	Invertible
$3_1\#3_1\#6_1^m$	Invertible
$3_1\#3_1^m\#6_1$	Invertible
$3_1\#3_1^m\#6_1^m$	Invertible
$3_1^m\#3_1^m\#6_1$	Invertible
$3_1^m\#3_1^m\#6_1^m$	Invertible
$3_1\#3_1\#6_2$	Invertible
$3_1\#3_1\#6_2^m$	Invertible
$3_1\#3_1^m\#6_2$	Invertible
$3_1\#3_1^m\#6_2^m$	Invertible
$3_1^m\#3_1^m\#6_2$	Invertible
$3_1^m\#3_1^m\#6_2^m$	Invertible
$3_1\#3_1\#6_3$	Invertible
$3_1\#3_1^m\#6_3$	Full
$3_1^m\#3_1^m\#6_3$	Invertible
$3_1\#4_1\#5_1$	Invertible
$3_1\#4_1\#5_1^m$	Invertible
$3_1^m\#4_1\#5_1$	Invertible
$3_1^m\#4_1\#5_1^m$	Invertible
$3_1\#4_1\#5_2$	Invertible
$3_1\#4_1\#5_2^m$	Invertible
$3_1^m\#4_1\#5_2$	Invertible
$3_1^m\#4_1\#5_2^m$	Invertible
$4_1\#4_1\#4_1$	Full
$3_1\#3_1\#3_1\#3_1$	Invertible
$3_1\#3_1\#3_1\#3_1^m$	Invertible
$3_1\#3_1\#3_1^m\#3_1^m$	Full
$3_1\#3_1^m\#3_1^m\#3_1^m$	Invertible
$3_1^m\#3_1^m\#3_1^m\#3_1^m$	Invertible

Chapter 10

Future Directions

The obvious next step in this theory is to generalize to the case of links. The first goal for developing such a theory is to understand how the prime decomposition of a link is ascertained from the JSJ-decomposition of the link complement. In the case of knots this is easy, you simply look at the JSJ tori which are adjacent to the knot compliment. The prime factors are the companions to the 3-cells which bound these tori and are opposite the knot complement. For links the situation seems to be much more complicated and it is not known what the analogous object to the prime decomposition tree (cf. Definition 53) should be. These objects must contain enough combinatorial information to encode which component of each prime link is involved in the connected sum. It is also unclear what group naturally acts on these objects in a analogous way to the action of $\Sigma(P)$ on $X(P)$.

It would also be interesting to look at the more general set of PD-codes whose associated surfaces are not necessarily spheres (or even non-orientable!). It is not hard to write down the Reidemeister moves as operations on PD-codes. Thus, one can rephrase knot theory fully in terms of PD-codes. Since PD-codes encode the information of an entire knot diagram including a surface on which it lives it seems likely that they could be used to develop a combinatorial knot theory in arbitrary 3 manifolds by looking at diagrams on the

middle surface of a Morse decomposition. There would be more "Reidemeister" moves that correspond to the ambiguity in flowing a knot to the middle surface. These new moves probably include sliding arcs over compressing disks to the middle surface. Such a theory would have interesting properties because knots that embed on the middle surface would be trivial from the perspective of PD-codes because they have no crossings! However, for sufficiently complicated diagrams it seems possible to define combinatorial knot invariants using these methods.

Chapter 11

Bibliography

[Ber12] Casey M.P.; Dannenberg E.; George W.; Johnson A.; Kelley A.; LaPointe A.; Mastin M.; Parsley J.; Rooney J.; Whitaker R. Berglund, M.; Cantarella, J. *Intrinsic symmetry groups of links with* 8 *and fewer crossings*, Symmetry, 4, 143-207. (2012).

[BN11] Dror Bar-Natan, *The knot atlas*, http://katlas.org/ (2011).

[Bud06] Ryan Budney, *JSJ-decompositions of knot and link complements in the* 3*-sphere*, L'enseignement Mathe'matique (2) 52 (2006).

[Bud07] ———, *Little cubes and long knots*, Topology, Volume 46, Issue 1, Pages 127 (2007).

[Can12] E.; LaPointe A. Cantarella, J.; Rawdon, *The shapes of tight composite knots*, Journal of Physics A, Issue 22 (2012).

[Cer68] J. Cerf, *Sur les diffeomorphismes de la sphere de dimension trois*, Lecture Notes in Mathematics, No. 53, Springer-Verlag, Berlin, 1968. (1968).

[CL11] J. C. Cha and C. Livingston, *Knotinfo: Table of knot invariants*, http://www.indiana.edu/ knotinfo (2011).

[Has58] Y. Hashizume, *On the uniqueness of the decomposition of links*, Osaka Math J. (1958).

[Joh79] K. Johannson, *Homotopy equivalences of* 3*-manifolds with boundaries*, Lecture Notes in Mathematics, 761. Springer, Berlin (1979).

[JS76] W. Jaco and P. Shalen, *A new decomposition theorem for irreducible sufficiently-large* 3*-manifolds*, Algebraic and geometric topology (Proc. Sympos. Pure Math., Stanford Univ., Stanford, Calif.,1976), Part 2, pp. 7184, Proc. Sympos. Pure Math., XXXII, Amer. Math. Soc., Providence, R.I. (1976).

[Kau11] Louis H. Kauffman, *Introduction to virtual knot theory*, http://arxiv.org/abs/1101.0665 (2011).

[Sch53] H. Schubert, *Knoten und vollringe*, Acta. Math (1953).

[WCW69] Jr. W. C. Whitten, *Symmetries of links*, Transactions of the American Mathematical Society, Vol. 135. (Jan., 1969), pp. 213-222. (1969).

[WN97] G.A. Swarup W. Neumann, *Canonical decompositions of* 3*-manifolds*, Geometry and Topology (1997).